NORTH COAST RIVER LOADING STUDY
ROAD CROSSING ON SMALL STREAMS
VOLUME II. STRESSORS ON SALMONIDS

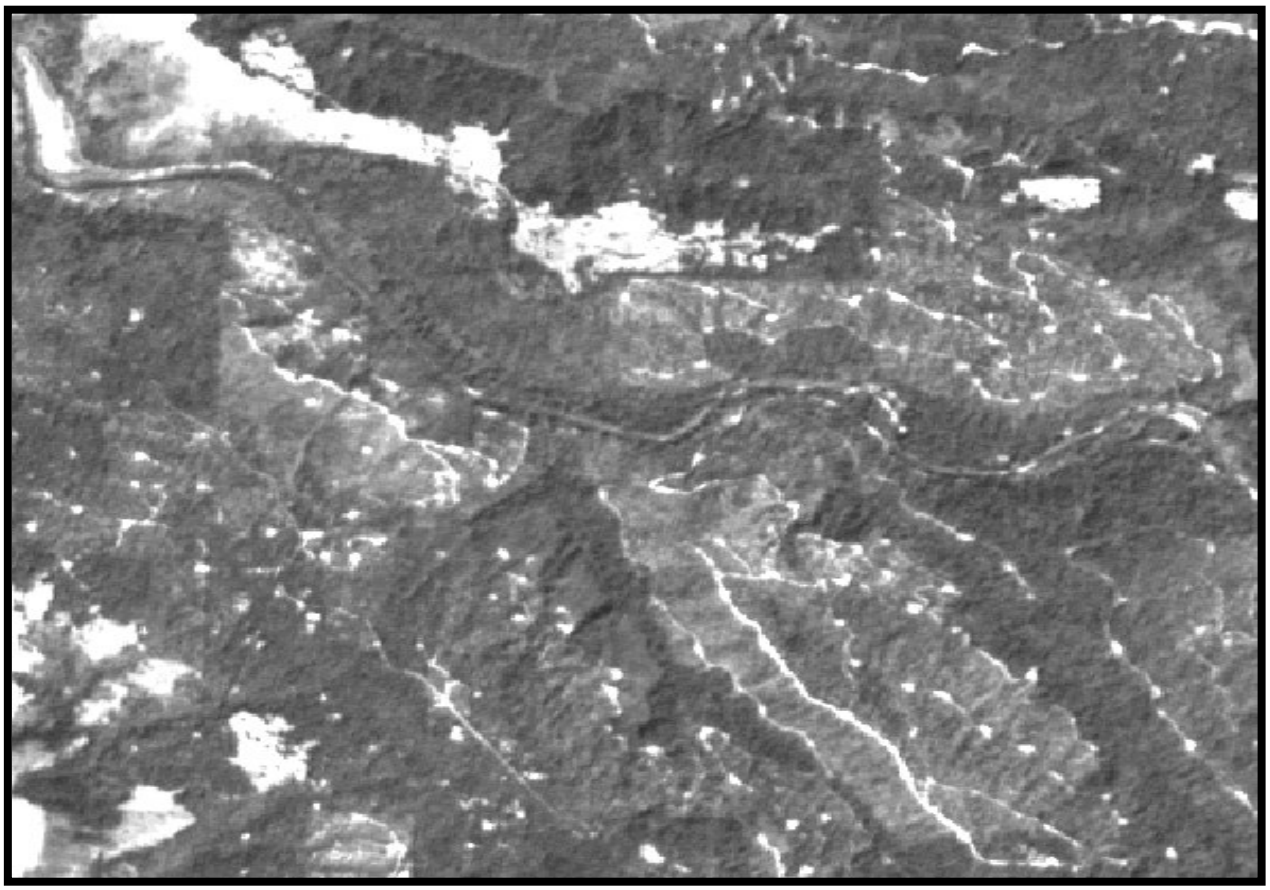

A REPORT PREPARED FOR THE
DIVISION OF ENVIRONMENTAL ANALYSIS
CALIFORNIA DEPARTMENT OF TRANSPORTATION
INTERAGENCY AGREEMENT NOS. 43A0014 AND 43A0073

MICHAEL L. JOHNSON

JOHN MUIR INSTITUTE OF THE ENVIRONMENT
UNIVERSITY OF CALIFORNIA, DAVIS

GREGORY PASTERNACK, JOAN FLORSHEIM, INGE WERNER, TIMOTHY B. SMITH, LIZABETH BOWEN, MELISSA TURNER, JOSH VIERS, JEFF STEINMETZ, JOSE CONSTANTINE, ERIC HUBER, OSCAR JORDA, JOAQUIN FELICIANO

CTSW - RT- 02 - 040
OCTOBER 2000

Caltrans

LIST OF TABLES

LIST OF FIGURES

STRESSORS ON STEELHEAD AND COHO

Several stressors could have been, and could still be responsible for the decline of species of anadromous fish in the Navarro watershed. The two abiotic stressors that are the focus of current regulatory action are sediment and high water temperatures. An additional abiotic stressor that might impact salmonid populations is nonpoint source contaminant inputs to the system. These inputs can result from runoff from highways, inputs from urban centers (no buildings are on septic systems), and agricultural nonpoint inputs. These can act singly and can interact synergistically to keep both steelhead and coho numbers far below historical levels. In addition, these stressors can interact with biotic stressors such as competitors and predators to further reduce the number of individuals at sites across entire watersheds. To determine the relative impact of various stressors on current populations of anadromous fish, we examined the three primary abiotic stressors, sediment, temperature, and water quality, and the two primary biotic stressors, predation and competition.

Sediment in the Navarro River watershed

Long-term sediment deposition

Small rivers in tectonically active regions deliver a disproportionate amount of sediment to the oceans relative to the area they drain (Milliman and Syvitski 1992). The abundant sediment deposited off shore and at the mouths of mountainous streams provides an unique opportunity to extrapolate the depositional history to infer the primary controls of basin evolution (Wheatcroft et al. 1996, Wheatcroft et al. 1997, Pasternack et al. 2001). Although the sedimentary record at the mouths of small, mountainous streams is extensive, the majority of sediment carried by them is actually deposited upstream from the basin mouth (Trimble 1977, Ichim 1990, Milliman and Syvitski 1992, Mertes and Warrick 2001). As a result, it is worthwhile to examine the record of overbank deposition preserved in

floodplains in order to examine changes in basin sediment storage as a response to environmental change (Walling et al. 1996, Owens and Walling 2002).

Basin storage, via overbank deposition, is considered to be sensitive to environmental change (Trimble 1977, Meade 1982, Walling 1983), which produces changes in sediment transport. Many techniques have been used to study sedimentation rates in floodplains: sediment traps (e.g., Gretener and Strömquist 1987, Asselmann and Middelkoop 1995), post-flood surveys (*e.g.,* Gomez et al. 1997), and coring in conjunction with radioisotopes (commonly ^{210}Pb and ^{137}Cs) (*e.g.,* Nicholas and Walling 1997, Goodbred and Kuehl 1998). The episodic nature of flooding in small, mountainous streams makes sediment traps and post-flood surveying impractical because of the time lag between flood events and the inability to accurately predict flood occurrences. Although radioisotopic studies of accretion rates have achieved general success, the technique is limited in narrow, densely forested valleys because the rate of atmospheric deposition of an isotope is either unknown or decreased due to leaf interception (Ritchie and McHenry 1990). Furthermore, the relatively short half-lives of commonly used radioisotopes makes them very useful in determining short-term (decadal to centennial) sedimentation rates, but not in establishing long-term (centennial to millennial) deposition rates. In order to avoid the complications of the above techniques, an overbank sedimentation study within a narrow, forested floodplain may be limited to the identification of datable horizons in floodplain cores (*e.g.,* Costa 1975, Trimble 1983) and/or the use of microfossils (*e.g.,* Brush et al. 1982, Brown 1988). However, the complications involving microfossil preservation on floodplains (Brown

1996) may make the identification of datable horizons the only means of establishing long-term rates of overbank deposition in a narrow, forested valley.

Simply measuring rates of overbank sedimentation on any particular floodplain may not be enough to understand the relationship between sediment storage and environmental change in a small, mountainous catchment. In general, sediment yield increases with decreasing stream order (Trimble 1977, Ichim 1990) and differences in sediment yield across stream orders may result in different responses to environmental change across the drainage basin (Graf 1983). As a result of spatial variance in sediment yield, it can be expected that rates of overbank deposition on floodplains adjacent to different stream orders will be different as well. Although some studies (Walling et al. 1996, Walling and He 1998) found no significant downstream trend in overbank deposition rates, examining changes in sedimentation as a function of stream order may provide insight about the variability of sub-basin response to environmental change.

This study reports long-term sedimentation rates in the Navarro River drainage basin of Northern California (Figure 1-1, Vol. I) using ^{14}C geochronology. Rates are reported for four floodplains adjoining streams of different stream orders. The long-term sedimentation rates across different stream orders provide the means to generalize the spatial and temporal responses of the Navarro River basin to varying forms of land use. Although there are significant data to suggest that alteration of the landscape by deforestation (*e.g.,* Gresswell et al. 1979), vegetation conversion (*e.g.,* Rice et al. 1969), and road construction (*e.g.,* Megahan and Kidd 1972) increase sediment input into streams, it is not understood

how these variables interact with climate and tectonics to influence denudation and sediment-transport patterns. This study attempts to determine whether climate, tectonics, or land-use change is the principal control on floodplain evolution within the Navarro River drainage basin. The results of this study may aid in understanding the extent to which the Navarro River drainage basin has been impacted by land-use change.

Natural Setting

Based on USGS gauge (11468000) measurements since 1950, Navarro River discharge typically ranges from near zero to 185 $m^3 s^{-1}$ with peak discharges in March and April. Based on the same data source, from November 1998 to March 2001 suspended-sediment load ranged from 4.10 to 24600 t day^{-1}. Suspended sediment-grain size data from November 1998 to March of 2001 indicate that on average, 68% of the sediment was finer than 0.0625 mm, with the remaining fraction finer than 2 mm.

Elevations within the basin range from 0 to 1100 m above sea level. Drainage of the Navarro River parallels the San Andreas fault-zone located 20 km to the southwest of the watershed. As a result of the convergence at the Mendocino Triple Junction, approximately 100 km to the north, uplift rates in the region are on the order of ~0.3 mm yr^{-1} (Merritts and Bull 1989). Most of the basin is underlain by Coastal Belt rocks of the Franciscan Formation that contain highly deformed sandstone, shale, and minor fractions of volcanics, limestone, and conglomerate (Bailey et al. 1964).

Three nested floodplain areas represented by four sediment cores were chosen within the watershed for detailed analysis. Study site NRWS-09 was in a floodplain wetland at the mouth of Flynn Creek, a 4th-order stream that drains 19.3 km^2. Because Flynn Creek is several orders smaller than the stream it flows in to, it may experience a significant backwater effect that promotes deposition of its sediment during floods in the area where the core was collected. Site NRWS-04 was situated in a floodplain of the North Fork, a 5th-order stream that drains 182.7 km^2, including the drainage area of NRWS-09. Sites NRWS-02 and NRWS-03 occurred in a floodplain on the mainstem of the Navarro River, a 7th-order stream that empties directly into the Pacific Ocean. The mainstem sites had an upstream drainage area of 776.1 km^2 and 789.4 km^2, respectively. All study locations were located away from low-order channels and impinging alluvial fans as described by Florsheim and others (2001).

Methods

Field and Lab Procedures

Four sediment cores were collected using two different technologies suitable for the field conditions. Three cores were collected from floodplain sites located on outer meanders of the Navarro River and the North Fork using a Geoprobe 66DT drill-rig at sites NRWS-03 (1063 cm depth), NRWS-02 (1644 cm depth), and NRWS-04 (1383 cm depth) respectively. The Geoprobe 66DT collects a 5.08 cm diameter sediment core in discontinuous 122-cm sections within a protected outer casing that maintains the hole throughout the coring process. Because the Geoprobe was limited to accessible sites, the floodplain wetland at the mouth of Flynn Creek (site NRWS-09) was cored using a portable vibracorer. A single 7.62-cm diameter core was collected using an aluminum tube to a depth of 345 cm.

All cores were analyzed using a standard protocol based on the existing literature. Cores were opened in the laboratory and given standard stratigraphic examination for color, grain size, texture, and visible mineralogy. Cores were subsampled at 5-cm intervals for Geoprobe-collected cores and 3-cm intervals for vibracorer-collected cores. Bulk density was determined by weighing the known volume of the cylindrical sediment subsamples. Each subsample was then homogenized and stored in a temperature-controlled environment at 4°C. Approximately 1 g of sediment from each core interval was analyzed for water content by drying and organic content by loss-on-ignition during 5 hours at 550°C.

Approximately 30 g of material from each core interval was used for grain size analysis. Organics were removed from samples using 30% H_2O_2 (*e.g.,* Black 1965). Afterwards, the sediment was separated by wet sieving at 63.5 μm. The sand and gravel fractions of the dried >63.5 μm material were determined with a Tyler Ro-Tap sieve shaker using 2 mm, 1 mm, 0.5 mm, 0.25 mm, and 125 μm mesh sizes at 15 minutes per sample. The silt and clay fractions of the <63.5 μm material were determined using a Coulter LS230 Laser Particle Granulometer. Organic material that could be visibly identified was sent to Beta Analytic Inc. (Miami, FL) for ^{14}C dating. All dates reported in this study are conventional radiocarbon ages expressed as years before present (ybp).

Data Analysis

Core stratigraphy and grain size fractions were the primary data used to distinguish the potential mechanisms for sediment deposition within distinguishable zones in the core from each site. Deposition mechanisms may have included direct landslides, debris flows, lateral-accretion, and overbank flooding. Even though sites were carefully selected to

avoid the possibility of the first two as contributors, cores were carefully checked for any evidence of their presence, such as poor sorting and angular rock fragments. Sedimentary strata dominated by sand and gravel were interpreted as resulting from lateral-accretion. Because point bars in channels and near-channel overbank deposits have similarities in grain size distributions (Wolman and Leopold 1957, Nanson 1980), strata dominated by sand and having no gravel could represent either of the two settings. Stratigraphic analysis was used to best distinguish between strata of fluvial or floodplain origins. Sedimentary strata generally dominated by fines (defined hereafter as the sum of the silt and clay fractions) were interpreted as resulting from overbank deposition.

A chronostratigraphic sequence of all cores was developed based on determined ^{14}C ages and long-term average sedimentation rates within each depositional zone were determined on the basis of linear interpolation of radiocarbon dates. Date inversions were interpreted as indicative of particulate carbon stored upslope and subsequently transported to the final depositional site. The only alternative to this would be to assume that younger particulate carbon was moved down-core, but this interpretation was not viable as sedimentary strata showed no signs of vertical disturbance. Consequently, date inversions were eliminated and the youngest, basal dates were used to construct time-lines.

Results

Stratigraphy and Interpretation: Core NRWS-03

Core NRWS-03 showed some zonation in grain size and bulk density, but not in organic content. In Zone I, from 0 to 400 cm, sediment texture had a mean % sand of 46 and showed great fluctuations, ranging from 13% to 84% sand. Zone II occurred from 400 to

860 cm and showed a similar mean % sand as Zone I (52%) with nonperiodic fluctuations between 26% and 75% sand. Zone III occurred between 860 and 1063 cm and was marked by % sand increasing upward to a peak of 66. Fine sediment dominates the section of Zone III from 900 to 1063 cm.

In contrast to the fluctuating nature of the grain size in NRWS-03, bulk density had a distinct zonation, likely due to sediment consolidation at depth. Bulk density averaged 1.22 g cm^{-3} (±0.15 g cm^{-3}) between 0 and 200 cm. Below that depth there was a sharp increase in bulk density from 200 to 300 cm. From 300 to 1063 cm, bulk density was 1.81 g cm^{-3} with a smaller variation of ±0.11 g cm^{-3}. Peaks in bulk density did not necessarily correspond with peaks in sand content or organic content and thus represents a change in the amount of pore space that is likely a result of compaction due to overburden stress or to the position of strata below the water table where pores are filled with water rather than air.

Organic content in NRWS-03 was nearly constant through depth, averaging 4.25% (±1.02%). The lack of a trend in organic content as a function of depth implies that the amount of organic material preserved has not changed through time and supports the use of downcore comparisons. The relatively uniform organic content and grain size data sets imply that the depositional setting at the site of core NRWS-03 has not changed significantly through time and that the entire core is representative of a floodplain setting dominated by overbank deposition. Variations in sand content are interpreted to either represent changing proximity of the channel to the coring site or variations in flood

magnitude. Both processes could increase the competence of water flowing over the floodplain in the vicinity of the coring site and thus change the sand content.

Stratigraphy and Interpretation: Core NRWS-02

Core NRWS-02 showed two zones of fluctuating sand and fines. In contrast to core NRWS-03, the bottom of core NRWS-02 contained gravel. Zone I occurred between 0-725 cm depth and the mean sand content in this top zone was 55% (±14%). Large-amplitude variations of 25-75% were evident in sand content in this zone, similar to the upper 400 cm of core NRWS-03. Zone II occurred between 725-1210 cm and was composed of a highly uniform sequence of sand-dominated horizons with a mean content of 76% (±8%). Zone III was a coarsening upward sequence between 1210-1640 cm that transitioned upward into interchangeable gravel-dominated/sand-dominated horizons between 1175-1450 cm depth.

The bulk density profile of core NRWS-02 showed gradual compaction near the top that is followed by random variations. The bulk density in the top 200 cm averaged 1.37 g cm^{-3} (±0.24 g cm^{-3}). Below that it was 1.87 g cm^{-3} (±0.23 g cm^{-3}) down to the bottom. The average in the lower zone was very close to that for core NRWS-03.

The organic content profile of core NRWS-02 showed a slight decrease with depth except for three large spikes. The mean organic content for the core was 3.06% with a standard deviation of 1.65% excluding the three spikes. Organic content decreased slightly through depth from a high of 6.40% at the top to a low of 2.21% at 1500 cm depth. Large spikes in organic content, as high as 32%, were found between 1050 and 1300 cm. In this interval,

the organic material was comprised mostly of large (length >30 mm) wood fragments, whereas the rest of the core had small (diameter <7 mm) charred wood fragments or microscopic organic material. The timing of the spikes corresponds with the transition from the gravelly Zone III to the sand-dominated Zone II.

The grain size classes and variations observed throughout Zone I are similar to what was observed in core NRWS-03 and are interpreted to be a result of overbank deposition. Although the sediment of Zone II was coarser than that of Zone I, it is not possible to discern whether it was a result of overbank-levee deposition or was of fluvial origin, representing a bar deposit. Zone III is interpreted to be channel bed or bank deposits stemming from lateral-accretion. The sub-rounded to rounded shape of the grains of Zone III support a fluvial rather than colluvial origin. Based on the interpretation, the only deposits that could be confidently interpreted as overbank floodplain deposits were of Zone I.

Stratigraphy and Interpretation: Core NRWS-04

Three zones were evident in core NRWS-04 based on grain size data. Zone I occurred between 0 and 646 cm depth and was characterized as a fining upward sequence. The mean sand content of this zone was 59% (±12.9%) fining upward from a value of 72.2% to 46.5%. Zone II occurred between 646 and 1100 cm and was defined as coarsening upward from the base to a gravel-dominated sequence between 890 and 970 cm. From 646 to 890 cm, Zone II was a fining upward sequence with a short, but significant spike in the gravel

fraction at the topset. Zone III occurred from 1100-1383 cm depth and was a fining upward sequence from gravel-dominated to sand-dominated horizons.

Similar to core NRWS-02, bulk density increased significantly from the surface to 205 cm due to compaction, but then leveled off. Bulk density averaged 1.31 g cm^3 (±0.24 g cm^3) between 0 and 2.0 cm and 1.82 g cm^3 (±0.22 g cm^3) between 205 and 1380 cm. These averages were highly consistent with those observed in NRWS-02 and NRWS-03.

The organic content of sediment in core NRWS-04 was relatively uniform through depth. The whole-core average was 2.95% (±1.19%). A slight decrease was evident from the surface through the first meter.

The grain size pattern in Zone I was very similar to those observed in core NRWS-03 and in Zone I of core NRWS-02, indicating that it is the result of overbank deposition. The gravel of Zone II contained sub-rounded to well-rounded grains, which indicate lateral-accretion. A channel bank or bed is the likely depositional setting for the sediment of Zone II. The gradual fining upward in this zone was in contrast to the abrupt change observed in core NRWS-02 and is interpreted to represent a point bar. The sediment of Zone III was more variable than that of Zone II, yet contained sufficient amounts of gravel to imply a period of lateral-accretion. The variability in Zone III may have been a result of deposition onto a surface away from the channel thalweg, such as onto a bar. Based on the grain size data, the only zone that represented overbank deposits was Zone I.

Stratigraphy and Interpretation: Core NRWS-09

The grain size data of core NRWS-09 was rather uniform through depth and was characterized by horizons dominated by fines (52-81%). Bulk density showed no significant trend through depth and averaged 1.64 g cm^{-3} (±0.28 g cm^{-3}). However, two trends were apparent based on the organic content data. Organic content decreased from 0 cm through the first 20 cm and remained uniform through 190 cm. The average from 20-190 cm was 4.58% (±1.43%). Between 190 and 350 cm, organic content was highly variable (3-18%) and averaged 4.58%. The differences in trends may be due not only to the quantity, but also the nature of organic material preserved in the core. Organic material was more diffuse with visible charred remains <10 mm in diameter from 0 to 190 cm, whereas large woody fragments (length >70 mm) made up most of the organic material from 190 to 350 cm. Several of these wood fragments were AMS dated. A deposit of wood can greatly affect the measure of organic content of a sediment sample with fixed volume, thus the organic content data below 190 cm should be analyzed with this effect in mind. Whether the increased deposition of wood was due to a change in depositional setting or to a change in upstream land cover and sediment supply is unknown. Although organic content varied with depth, grain size remained uniform throughout core NRWS-09, implying that the backwater wetland depositional setting has persisted through the recent past.

Long-term Average Sedimentation Rates

The chronostratigraphic sequence of all cores showed significant differences in deposition rates through space and time. Dates that were not included in the stratigraphic interpretation of the cores because of inversions were the 3040 ±40 ybp, 4470 ±50 ybp

dates for core NRWS-04 and the 2230 ±40 ybp date for core NRWS-09 for reasons described in the Methods. Since no date was measured to construct a '2000 ybp' time-line for core NRWS-02, a time-line was interpolated based on the '3000 ybp' horizon and dates from cores NRWS-03 and NRWS-04.

Comparing cores NRWS-04, -02, and -03, the thickness of sediment bounded by time horizons decreased in the downstream direction, implying that sedimentation rates did the same. Core NRWS-09 did not show such trends, suggesting that the differences may be due to sub-basin characteristics that affect sedimentation rates at this site.

A distinction must be made of the mode of sedimentation responsible for any given horizon within the cores. As a result, net-averaged overbank and lateral-accretion rates have been constructed based on ^{14}C dates. The range of sedimentation rates possible based on the standard error measured in the conventional radiocarbon ages is presented in Table 3. Several trends are apparent, the first of which is that sedimentation rates decreased from the mid-Holocene to the present. The second trend is that sedimentation rates decrease in the downstream direction from site NRWS-04, which occurs on the 5th-order North Fork, to sites NRWS-03 and NRWS-02, which occur on the 7th-order Navarro River. Although changes in the location of the channel relative to the core sites can influence rates of overbank accretion, the similarity between cores NRWS-03, -02, and -04 indicates that changes in overbank accretion rates are rather due to changes in some geomorphic characteristic in the Navarro basin. A third trend is the significantly larger net-lateral-accretion rate for core NRWS-04. Although averaging through depth underestimates the

complexities of fluvial sediment deposition, the rate established for core NRWS-04, a value of 1.81 cm yr^{-1}, is comparable to the rates found by Goodbred and Kuehl (1998) (>1.47 cm yr^{-1}) in a tectonically active setting. The net-averaged overbank deposition rates found for all cores, ranging from 0.074-0.563 cm yr^{-1}, are also similar to rates calculated in floodplain studies in lowland settings (Ritter et al. 1973, Orbock-Miller et al. 1993, Walling and He 1998) and in tectonically active settings with larger drainage areas (>10000 km^2) (Allison et al. 1998, Goodbred and Kuehl 1998), but are much less than those found by Gomez and others (1999) in a tectonically active setting with a comparable drainage area (~2000 km^2).

The sedimentation record for core NRWS-09 is more complex than the records of other cores. The complexity may be a result of the finer sampling resolution for ^{14}C dating so that the ability to measure the variability of sedimentation is improved. Based on the overbank deposition rates, a significant increase in sedimentation occurs between 860 and 1250 ybp, from 0.085 cm yr^{-1} to 0.344 cm yr^{-1}. The average rate declines from 170 through 860 ybp to 0.094 cm yr^{-1}. Sedimentation rates increase moderately from 170 ybp to the present to a value of 0.141 cm yr^{-1}. If the variations observed in sedimentation are real measures of differences in sub-basin-sediment loading and if those variations altered sediment loads within the North Fork sub-basin and/or the Navarro basin, the absence of variations within cores NRWS-03, -02, and -04 may be due to averaging over longer time-intervals than in core NRWS-09.

Discussion

Perspective on Floodplain Sedimentation

The organic content, bulk density, and grain size data sets have allowed confident interpretation of core sediment of floodplain origin and have provided a framework from which to analyze sedimentation rates. Whether by constructing floodplain sedimentation rates through temporal averaging or by event-based data, many studies have observed that overbank deposition rates decrease through time (Walling et al. 1996, Gomez et al. 1999). Gomez and others (1999) provide suggestions explaining why the phenomenon may occur: (1) the long-term accumulation of sediment decreases the connectivity of the floodplain with the channel thereby decreasing flood frequency; (2) deposition occurs as discrete centimeter-to-decimeter units in which low modern rates of accumulation are due to the lack of time required to deposit large volumes of sediment rapidly; (3) the effects of anthropogenic disturbance diminish through time. Although this study does not definitively lend support to a causal mechanism, it does provide further evidence for decreasing deposition rates through time within floodplains of small, tectonically active drainages. Records of anthropogenic activity and climate and tectonic data in the Navarro region provide an opportunity to examine controls on the evolution of floodplains in this context.

Anthropogenic Control of Floodplain Evolution

History of land use in the Navarro watershed is very recent. Although many forms of land use occur within the basin, logging activities have had the greatest impact in terms of magnitude of change. After settlement in the 1850's, *Sequoia* stands were gradually logged through the turn of the century (Palmer 1967, Holmes 1996), and an aerial photograph

documents that much of the North Fork basin was deforested by a wildfire and logging in 1936. A third cut of the North Fork basin began in the 1990's, the extent of which is undetermined (Mendocino Redwood Company 2000).

A number of studies provide data showing the increased likelihood for landsliding after logging (*e.g.*, Sidle et al. 1985) and support the ability of floodplains to record anthropogenic disturbance as increased overbank deposition (Knox 1987, Marron 1992). However, based on long-term, net-averaged sedimentation rates, it appears that floodplains in the Navarro basin have not experienced increased sedimentation caused by disturbances to the landscape, at least over the time scales investigated by this study.

There are many complications involved in trying to determine the controls of floodplain sedimentation based on net averages. In particular, averaging through a large depth interval could mask any effects of anthropogenic disturbance on overbank sedimentation. The best way to insure that the effects of change in sediment loading are measured is to subsample and date sediment cores at a high resolution, though this method is limited by the availability of organic material. Because of its relatively young dates, core NRWS-09 yields the best opportunity to examine anthropogenic effects on overbank deposition. However, sedimentation rates were much higher in the prehistoric section of the core, suggesting either that land use has had a minimal impact on sedimentation over hundred to thousands of years because the time necessary for recent land-use change to translate into sedimentation changes may have not transpired, or that floodplains in Flynn Creek have not recorded those impacts for reasons particular to the catchment itself.

The Flynn Creek floodplains may fail to record sediment pulses because the system of roads built over tributaries is storing sediment upstream. As is true for much of the North Fork basin, roads were built in the Flynn Creek catchment during logging periods to allow for the removal of timber. There are many cases in which bridges were built over tributaries with narrow culverts that maintained minimum discharge. Based on reconnaissance investigations, large volumes of sediment were deposited upstream of the culverts as a result of loss in stream competence. The amount of sediment transported into the tributary network as a result of logging and stored within the channels remains unquantified, but was quite large. Depending on the preservation of the historic bridges and culverts, historic sediment is now being released at a reduced but significant rate, as evidenced by deep incision above some culverts.

Another hindrance to sediment dispersal has been the damming effect of large woody debris stored in channels. In particular, Keller and others (1995) found that the mean area of debris-stored sediment within channels is much higher in disturbed settings affected by logging than undisturbed settings.

Work by Benda and Dunne (1997a,b) may provide reasoning behind the lack of an anthropogenic record in cores NRWS-03, -02, and -04. Benda and Dunne (1997a, b) describe that the frequency and magnitude of sediment-pulse events increase with drainage area. This results in a more continuous supply of sediment to higher-order streams and an overall dampening in the amplitude of sediment pulses. Although it is more difficult to

record sediment pulses in higher-order streams, one would expect that if anthropogenic disturbance is the principal control on sediment transport, then a marked increase in overbank deposition rates should be observed relative to the past. It is possible that the sediment produced by land-use change is being stored in the uppermost parts of the basin and that due to increased storage, such as was observed in Flynn Creek, any effect of land-use change in overbank deposition rates in higher-order streams has been dampened. Based on these observations, climate and tectonics may be the dominant controls on the evolution of Navarro floodplains over hundreds to thousands of years.

Climatic and Tectonic Control on Floodplain Evolution

Although climate and tectonic records of the Navarro region are generalized, they provide a framework from which to examine the effects on floodplain overbank deposition. Eustatic sea-level rise was fairly constant throughout the mid to late Holocene averaging between 0.4 and 0.7 mm yr^{-1} (Fleming et al. 1998). Average tectonic uplift has been relatively uniform throughout the Holocene and is approximated to be 0.3 mm yr^{-1} in the vicinity of the Navarro basin (Merritts and Bull 1989). The combined result of eustasy and tectonics has been relative sea-level rise ranging from 0.1 to 0.4 mm yr^{-1}. Because the effect of tectonics to lower base level is muted by sea-level rise, it is argued that the only geomorphic effect it has in the Navarro basin, at least through the Holocene, has been to randomly generate sediment pulses via earthquake-induced mass movements. In support of this argument, some studies show that intermediary- to high-order streams of the North Coast, California, are able to rapidly adjust and maintain local base level in response to uplift (Merritts and Vincent 1989, Snyder et al. 2000).

It is likely that the climate history of the Navarro basin followed a similar pattern to areas both north and south of the study site. Conditions in the latest Pleistocene were wetter and cooler than present in the Navarro region (Sea and Whitlock 1995, Grigg and Whitlock 1997, Mohr et al. 2000). In a study that describes climate for all of coastal California, Johnson (1977) states that a xerothermic period occurred between 8000 and 3000 ybp in which climate was warmer and drier. Data taken from Clear Lake, California, support Johnson's (1977) time frame for a xerothermic period (Adam and West 1983). Data from Sea and Whitlock (1995) and Grigg and Whitlock (1997) from western Oregon suggest that the xerothermic period occurred during a broader time frame, extending from about 10000 to 4000 ybp. Studies in the Klamath Mountains of California (Mohr et al. 2000) and in central-coastal California (Rypins *et al*., 1989) further support a xerothermic period that occurred after 10000 ybp. A cooling trend followed by increased precipitation occurred after 7000 ybp and increased after 4000 ybp until the present (Johnson 1977, Sea and Whitlock 1995, Mohr et al. 2000).

If the region's ability to generate sediment pulses by earthquakes has remained relatively constant in the past, then different climate scenarios would affect how capable stream networks were in moving sediment through the system. According to Rypins and others (1989), climate in the central coastal California region was marked by intense winter storms from 12000 to 10000 ybp. Intense winter storms may not only provide a mechanism for transporting a sediment pulse, they may also initiate mass-movement events (Page et al. 1994). Changes in climate also induce changes in vegetation structure and fire

frequency, both of which can adversely affect hillslope stability (Reneau et al. 1986, Benda and Dunne 1997a, Brown and Hebda 2002). Regardless of the mechanism, many studies document an increase in the frequency of landsliding in the late Pleistocence and early Holocene (Reneau et al. 1986, Rypins et al. 1989, Reneau et al. 1990). Personius and others (1993) further document increased stream and floodplain deposition during the late Pleistocene/early Holocene and suggest that the aggradation was a result of increased sediment loading from mass-wasting events. As the magnitude of storms subsided during the middle Holocene, one would expect overbank deposition rates to do the same as a result of the decreased ability of streams to transport sediment and the decreased production of colluvium. The overbank deposition rates observed in this study are part of a general declining trend in sedimentation during the Holocene as a result of decreased precipitation and an exhaustion of sediment supplies. After the end of the xerothermic period, the decline in overbank deposition rates continued due to the infrequency of high magnitude storms and a stabilization of the landscape by vegetation (Mohr et al. 2000), both of which combined to decrease the generation of sediment pulse events. Mohr and others (2000) cite evidence that at about 2000 ybp, conditions became similar to modern regional climate. The increased precipitation and cooling after 2000 ybp should have decreased the rate of overbank deposition. Based on our interpretation of the existing data, climate is the principal controlling factor of floodplain evolution in the Navarro basin during the Holocene.

Perspective on Floodplain Sediment Storage

It is well known that overbank deposition rates vary with distance from a channel (Asselman and Middelkoop 1995, Goodbred and Kuehl 1998, Walling and He 1998; Walling et al. 1998), and as such, there is much uncertainty involved when trying to extrapolate sedimentation rates from one location across a floodplain surface. As a result, the inability to characterize a floodplain, based on sedimentation calculated from one core, makes it very difficult to compare rates between floodplains in this study. However, trends apparent in the historical floodplain record may provide the basis to allow for general comparisons to be made. The overbank deposition rates determined by this study average through variations caused by temporal changes in sediment loading and by spatial changes in the distance from channel source to core location. Spatial changes, which occur independently in each floodplain, have the particular function of masking any sedimentation relationships the floodplains may have with each other. Thus, a simple test for inter-floodplain relationships in overbank deposition would be to determine if there are apparent trends between floodplains that are consistent through time. Of course, the greater the time span investigated in the study, the stronger the case can be made for an inter-floodplain relationship. In this study, the trend that overbank deposition rates decrease in the downstream direction is indeed consistent through time and provides the basis for inter-floodplain comparison for the Navarro basin. It must be mentioned that because of the large degree of uncertainty involved in comparing point calculations of sedimentation, more cores are necessary if the inter-floodplain relationship argued heretofore is to be considered truly sound.

Walling and others (1998) argue that floodplain sediment storage increases in the downstream direction. Floodplain size increases downstream and thus provides greater storage capacity, even if the amount of sediment carried by the channel declines due to upstream storage (Trimble 1977, Ichim 1990). The sedimentation data illustrated in Figures 8 imply that storage in the Navarro basin may actually be greatest in the intermediary channels rather than highest-order channels. Sedimentation rates at site NRWS-04 are nearly three orders of magnitude larger than at downstream sites and nearly an order of magnitude greater than the increase in floodplain-width downstream. This suggests that sediment storage is highest in the 5th-order North Fork due to reasons that may be unique to the Navarro drainage.

In the Franciscan Assemblage that underlies most of the Navarro basin, mass movements are a common occurrence due to the high weathering potential and the fractured nature of the bedrock (Kleist 1974, Kramer 1976). Although mass movements onto floodplain surfaces of higher-order streams occur within the basin (Sowma-Bawcom 1996), most slope failures occur in the 1st- or 2nd-order streams where relief is the greatest (Montgomery and Dietrich 1994, Dietrich et al. 1993). One explanation of the largest floodplain sedimentation occurring in the 5th-order North Fork is that it is simply more connected to the sediment-producing 1st- and 2nd-order streams and is capable of storing some portion of the introduced load into available floodplains. This being the case and holding all other variables constant, it can be expected that the effects of any sediment pulses produced in the lowest-order streams are dampened in the highest-order streams as a result of the time

required to transport the sediment and the storage capacity of the upstream channel network (Pearce and Watson 1989, Jacobson 1995, Benda and Dunne 1997b).

The ability of floodplains along the Navarro River to record sediment pulses may be further dampened by the lack of space available for floodplain growth. As the Navarro River meanders westward across the basin, it has to cut into marine terraces in order to continue toward the Pacific Ocean, leaving relatively little room for the river to migrate and build floodplains laterally. As a result, sediment pulses that occur throughout the basin may only have a measurable effect on overbank deposition in intermediary channels while the highest-order channels are only able to record longer-term changes in basin denudation rates. Considering the complexity of sediment routing and storage shown in this study, caution should be used when making basin-wide characterizations based on measurements of river-sediment yield at mouths or on coastal shelves.

Conclusions

Under pristine conditions, floodplains located along intermediary-order streams are more able to record the long-term effects of sediment pulse events than lower-order or higher-order streams in the Navarro basin. Low-order streams are where most sediment available for transport enters the system. Steep gradients and narrow valleys promote rapid flushing of the sediment to higher-order streams thus limiting floodplain accretion. The highest-order streams of the basin are constrained as a result of incision into marine terraces. Incision has prohibited space for lateral migration and floodplain growth, minimizing the ability of the highest-order floodplains to store sediment. Because of the complexity of sediment routing and storage, caution must be made when making basin-wide

generalizations from sediment yield measurements obtained at river mouths or coastal shelves.

Land-use change has not had a significant impact in altering long-term average overbank deposition rates in the Navarro basin. Land-use changes have occurred throughout the basin since the 1850's, with major portions of the basin being deforested completely during different periods. However, historic road-building activity has blocked many low-order valleys preventing the large quantity of logging-related sediment from escaping the lowest-order tributaries and settling on established floodplains. Thus, sedimentation rates were much higher in the past than the present for all sites, suggesting that climate and tectonics are the primary controls of the evolution of Navarro floodplains.

Climate is the principal control of floodplain evolution in the Navarro basin throughout the Holocene and is responsible for higher sedimentation rates in the past than the present. Intense rainstorms combined with tectonic activity likely generated a higher frequency of mass movements in the early Holocene and produced large volumes of sediment available for transport. A xerothermic period decreased the frequency of high-magnitude storms and decreased the ability of channels to transport sediment load resulting in decreasing overbank deposition rates throughout most of the Holocene. A hypothetical model is constructed to explain overbank deposition rate during the late Pleistocene and Holocene and may be extrapolated to northern coastal regions in California.

Short-term sediment deposition

Fluxes of water and sediment serve as the primary agents of landscape change in most watersheds. Under natural conditions, the spatial and temporal distributions of these fluxes are a product of climate, vegetation, soils, topography, and wildlife activities. On top of this natural system is overlaid a history of human activities, particularly those that have occurred since Europeans conquered the North American continent. Deforestation, intensive agriculture, mining, and urbanization have fundamentally changed many landforms and landform processes, including hill slopes, river channels, and floodplains (Trimble, 1974; Costa, 1975; Jacobson and Coleman, 1986; and Whitney, 1994). An important consequence of this dramatic landscape change has been significant alteration of the distribution, volume, and quality of riverine habitats in response to sediment loading. Although some studies have assessed the effects of individual land uses on geomorphic processes and riverine habitat, no clear understanding exists in regard to the cumulative impacts of land-use change.

The overall goal of the on-going and proposed geomorphic study of landscape evolution in the Navarro River basin is to piece apart natural and anthropogenic impacts to determine when and where land use really affected the system. This information is intended to serve as an important tool for assessing the state of physical habitat for fish and invertebrates as well as aiding habitat restoration efforts. To address the key questions regarding human impacts, fish habitat, and restoration potential, it is necessary to focus on the processes of sediment generation, transport and deposition. In a watershed, long-term hydrologic and geomorphic processes are manifest through patterns and rates of sediment accumulation. Sediment not only links different components of the landscape (e.g. wetlands, forests, hill

slopes, pastures, etc.), but also the biological, physical, and chemical constituents of a single component. For example, in a riparian wetland, fine sediment is brought in by floods and creates new surfaces for pioneer plant species. Sediment is often loaded with important nutrients and metals required to sustain life, but it also carries toxins and heavy metals indicative of different land uses and geologic source areas. Rates and quantities of sediment transport and deposition are primarily controlled by hydrodynamics, so sediment can be used to reconstruct past fluid mechanics.

A goal of the geomorphic work conducted for the Navarro project was to quantify components of a sediment budget and to identify temporal and spatial changes in sediment production, transport, and storage processes in the Navarro basin that are important for aquatic habitat. As the project proceeded, it became apparent that the exceptionally large number of sites available for the generation of sediment, and the reconstruction of the transport of sediment and the deposition of sediment would prohibit a complete assessment. Consequently, we focused our efforts in the North Fork of the Navarro and the Flynn Creek subwatersheds as locations to catalogue and reconstruct the historic deposition of sediment respectively because they contained both coho and steelhead populations.

Methods

We attempted to quantify sediment sources and mechanisms of erosion, and differentiate sources of sediment related to Highway 128 and sediment sources related to natural sources or other land uses in the North Fork basin. To investigate this problem, erosion sources were mapped in the North Fork from aerial photographs taken in 1984, 1996, and 2000. The length, width, and depth of erosional features along Highway 128 were measured in

the field, and volume is calculated as their product. The area (product of length and width) of features in the remainder of the basin was mapped from aerial photographs. An estimate of the volume of debris produced by these erosional features was calculated as the product of the mapped area and the depth of each feature. Field reconnaissance in the study area documented the variability in depths among erosional features. We used a range of minimum, average, and maximum observed depths in order to provide an order of magnitude estimate of the volume of material produced by erosional features.

Results

A total of 1,065 erosional features were identified in the North Fork basin related to land uses such as logging and associated road networks, while a total of 38 features were identified in road cuts along Highway 128 from Dimmick State Park to where Highway128 crosses the North Fork in the North Fork basin. Tables 2-1 and 2-2 report the depth and calculated volume of debris produced in the North Fork watershed by both sources. The delivery ratio, an estimate of the connectivity between the sediment eroded from these features and the channel network, of 66% is estimated for slides the North Fork basin. Because of the proximity of Highway 128 to the main channel and floodplain of the North Fork, the delivery ratio from these sources was estimated at 100%. However, debris removal immediately after a road-related slide may minimize this source of sediment (as was observed following a slide in a road cut above the main Navarro River channel in March 1999).

Results of this study suggest that the volume of sediment produced by erosional sources along the four mile length of Highway 128 within the North Fork basin account for a small fraction of the total volume of sediment produced by erosional sources related to other land uses or natural causes in the remainder of the North Fork basin.

Table 2-1. Summary of Sediment Volume Contributed by Erosion Sources in North Fork Basin related to land uses such as logging and associated road networks.

	Minimum Estimate		**Mean Estimate**		**Maximum Estimate**	
North Fork Basin	**Depth (m)**	**Volume (m^3)**	**Depth (m)**	**Volume (m^3)**	**Depth (m)**	**Volume (m^3)**
Total Erosion	0.75	1,605,350	2.0	4,280,920	4.0	8,561,840
Delivered to Aquatic System		1,059,530		2,825,410		5,650,815

Table 2-2. Summary of Sediment Volume Contributed by Erosion Sources in North Fork Basin related to Highway 128.

Highway 128	**Volume (m^3)**
Total Erosion	16,720
Delivered to Aquatic System*	16,720

Assuming no removal

After estimating the potential sediment load that could be delivered to the river in the future, we reconstructed the historical sediment deposition rates in the Flynn Creek watershed. A total of 8 sediment cores have been collected from floodplain sediments in

the Navarro River basin so far. Six of the cores were collected using a Geoprobe drilling rig. According to the standard drilling procedure for this instrument, cores were collected in 1.2-m segments using dual-tube technology that keeps the drilling hole open and intact while segments are extracted from increasingly greater depths. While the theoretical limit of drilling using this approach is ~30 m, the practical limit for drilling in a single day in the Navarro River floodplain sediments is ~15 m. The two remaining cores that were collected were retrieved from remote locations that were inaccessible to the drilling rig and were more suitable for coring with a vibracorer. Whereas Geoprobe cores are 5 cm in diameter and segmented every 1.2-m, vibracorer cores are 7.5 cm in diameter and continuous over the whole length of the core. One vibracorer core was collected on the floodplain adjacent to the Navarro River estuary while the other was collected at the outlet of Flynn Creek, which was almost completely deforested in the 1930s and that randomly turned out to have several of its branches selected in the experimental design phase of the project. We selected Flynn Creek because its small size allowed a relatively complete history to be developed with a relatively short core. Core samples have also been collected from the North Fork watershed and the mainstem of the Navarro River in the wetlands located near the estuary. Due to time and monetary constraints, these cores have not been analyzed, but they remain available for further analysis.

Sediment deposition rates

Although the increased-runoff and sediment-production effects of logging are well documented (Hibert 1969, Bosch and Hewlett 1982, Guthrie 2002, Likens et al. 1970), there is considerable uncertainty about how rapidly and to what extent the sediment is transported through the stream network (Lewis 1998). The paucity of reliable field-data

further complicates an understanding of the control on basin evolution that anthropogenic effects may have in relation to climate and tectonics. Because much of the sediment produced is stored within a basin (Trimble 1977, Milliman and Syvitski 1992, Mertes and Warrick 2001), many studies now focus on floodplain sedimentation as a means of determining geomorphic response to environmental change (Asselman and Middlekoop 1995, Wallig et al. 1997, Goodbred and Kuehl 1998). Current methods used to determine rates of floodplain sedimentation, however, do not provide high-resolution data over varying temporal scales necessary to understand the importance of anthropogenic effects on the landscape. Here we uniquely apply a palynological approach to determine high-resolution overbank-deposition rates in a small, mountainous catchment impacted by logging. We show that overbank deposition rates respond to logging events within years of the onset of disturbance and increase over an order of magnitude from pre-disturbance rates. Over the time-scale investigated, the pre-settlement forest structure has not recovered, with much of the canopy replaced by disturbance-tolerant species. Our record shows that logging impacts sediment processes to a significantly greater level than natural controls over annual to centennial time-scales. Our technique could be used to improve environmental management of basins in light of the unique land-use history experienced by each.

The Flynn Creek basin (Figure 2-1), draining ~19.3 km^2 of mixed-conifer forest predominated by *Sequoia sempervirens* and *Pseudotsuga menziesii*, is located within the tectonically active Navarro watershed of coastal northern California. We chose the fourth-order Flynn Creek basin as the study site because its small size and steep drainage would minimize sediment storage and thus promote transport of sediment pulses through the system. Study of the Flynn Creek catchment, located within the Navarro watershed, is

important because the watershed represents the southernmost extent of natural-spawning ground for the endangered *O. kisutch*. Intensive land use and the highly erodible nature of the underlying Franciscan Complex have led the Environmental Protection Agency to establish strict sediment regulations for the Navarro basin in an effort to protect spawning habitat for *O. kisutch* and the threatened *O. mykiss* (USEPA 2000). Historically, land use in the Flynn Creek basin was dominated by logging activities, which principally targeted *Sequoia* stands. Although the extent of the first period of logging, which began in the 1850's (Palmer 1967, MRC 2000), is unclear, photographs document that a second period of logging and a 1931 wildfire completely deforested the basin by 1936 (Fig. 2-2a), and that a third-generation forest developed by 1998 (Fig. 2-2b). A third cut of *Sequoia* stands began in the region during the late 1990's (MRC 2000).

We chose a wetland floodplain near the mouth of Flynn Creek as a coring location (Fig. 2-1) because increased inundation frequency and its location at the end of the channel network allows the site to more fully integrate upstream geomorphic processes as overbank deposition. A vibracore was taken from the site to a depth of 350 cm, and the top 87 cm was examined for this study. After collection, the core was soon moved to a laboratory, analyzed for physical properties, and subsampled in 3-centimeter intervals for palynological analysis (Faegri and Iverson 1975). Two wood samples were removed at 24 cm and 87 cm depth and sent to Beta Analytic, Inc. (Miami, FL) for accelerated mass spectrometry radiocarbon dating. The conventional radiocarbon ages for the upper and lower samples were 170 ±40 ybp and 840 ±50 ybp respectively. The equation we used to obtain short-term overbank deposition rates was

$$R_i = \left(\frac{\bar{n}}{n_i} \right) \cdot \bar{R} \qquad (1)$$

where R_i (cm yr^{-1}) is the sedimentation rate of interval *i*, $\overline{n}$ is the average number of pollen grains per unit area of the interval *i*, n_i is the total number of pollen grains per unit area in interval *i*, and $\overline{R}$ (cm yr^{-1}) is the average sedimentation rate based on the radiocarbon dates (Faegri and Iverson 1975, Brush 1989, Brush 1984). This technique has proved very successful in comparison with the ^{210}Pb-based approach of determining sedimentation rates (Brush et al. 1982) and subsequently in inverse modeling of land-use change based on deltaic sedimentation (Pasternack et al. 2001). The pollen-based approach has two important advantages over the more commonly used ^{210}Pb- and ^{137}Cs-approaches (Walling et al. 1992, Walling et al. 1997, Goodbred and Kuehl 1998, He and Walling 1996) in that it can accurately record processes over hundreds of years without the limit of a short radioactive half-life and that it yields high-resolution temporal variations in sedimentation rates, not just averages.

Overbank deposition rates between 1188 and 1850 cal AD average 0.094 cm yr^{-1}, 50% less than the average of 0.141 cm yr^{-1} from 1850 to the present (Fig. 2-4a). Whereas sedimentation rates pre-1850 are rather uniform, rates post-1850 show large and frequent variations as high as 2.14 cm yr^{-1}, a value that is extremely high compared with rates found in much larger basins (Walling et al. 1992, Walling et al. 1997, He and Walling 1996, McDowell et al. 1990). Although the increase in average sedimentation post-1850 is informative, the palynological technique allows us to further analyze the depositional regimes responsible for the increase. For example, without the high-resolution rates that the technique allows us to calculate, it would be impossible to determine whether an increase in average sedimentation was caused by a step increase with consistently low rates before and high rates of deposition after land disturbance (Brush et al. 1982) or by episodic sediment pulses resulting from periodic land-use change.

The non-parametric Mann-Whitney U-test is based on rankings and thus, can statistically distinguish between a step change and a series of sediment pulses. In this context, a step change is defined as consistently high rankings after land disturbance and a series of sediment pulses as an intermix of rankings through time yielding no statistically significant difference between rates before and after disturbance. For our data set, the Mann-Whitney U-test ($\alpha = 0.01$) yielded a p-value of 0.277, therefore we rejected the null hypothesis that a statistically-significant step change is responsible for the increase in average sedimentation post-1850. The result of the test supports the hypothesis that logging practices have produced sediment pulses that travel rapidly through the Flynn Creek basin and implies that the system rapidly responds to and recovers from disturbance given enough time between logging periods. This is further evidenced by our high-resolution sedimentation data in that after 1850 and 1930, overbank deposition increased by as much as 7 and 13 times, respectively, before declining to rates slightly lower than antecedent conditions (Fig. 2-3a). Rapid return to antecedent conditions is likely a result of exhaustion of upstream sediment supply and/or hillslope stabilization by forest regrowth. More environmentally sound measures have been taken during the third cut of the Flynn Creek basin (MRC 2000); however, overbank deposition rates appear to have increased nonetheless (Fig. 2-3a).

If the percentage of load stored at the study site was rather uniform through the time period investigated, then our sedimentation data indicate that the Flynn Creek basin is able to transport large volumes of sediment rapidly to higher-order drainages. If a number of low-order basins are severely impacted in the same period, then sediment loads are likely to increase at such a rate that the sediment-transport abilities of higher-order streams will be compromised. Residents of the Navarro watershed affirm this problem and describe 4 to 5 m of in-channel accretion over the past 60 years along reaches of the 6th-order Navarro River. To protect habitat quality, land-management strategies need to be focussed on curtailing rapid land-use change in the most sensitive, low-order drainages.

Pollen data verify that sedimentation at the study site records the effects of land use and further documents the effects of logging in the Flynn Creek region. The relative pollen abundance of *Sequoia* declines from an average of 31.0% pre-1850 to 14.6% post-1850 (Fig. 2-3b). *Alnus*, which is often an indicator of disturbance conditions (Davis 1973), increases from 0.28% pre-1850 to 2.0% post-1850 (Fig. 3c). To determine whether the average changes in pollen were significant for both species, the Mann-Whitney U-test (α = 0.01) was used to test the null hypothesis that there was no significant difference between pollen abundance before and after 1850. In both cases, the null hypothesis was rejected based on a p-value of 0.0017 for *Sequoia* and of 0.0027 for *Alnus*. Therefore, even though sediment loading recovered to near-normal levels after logging, the forest composition changed significantly and shows no trend towards return to antecedent conditions.

Because anthropogenic disturbance affects many geomorphic processes, which occur at varying time scales (Kirtchner et al. 2001), it is difficult to ascertain its influence on geomorphic evolution in relation to climatic and tectonic controls. With the palynological approach, it is possible to obtain a consistent, high-resolution record over long enough time periods to reveal anthropogenic, climatic and tectonic effects. It is clear that overbank deposition rates observed during modern times in the Flynn Creek basin are far greater than any rate observed over the thousand-year record, suggesting that at annual to centennial time scales, anthropogenic disturbance may be so severe that it becomes the dominant control on floodplain evolution and perhaps on denudative processes. We advocate use of this method as a tool for watershed assessment throughout logging-impacted regions to quickly determine the scope of degraded watershed environments.

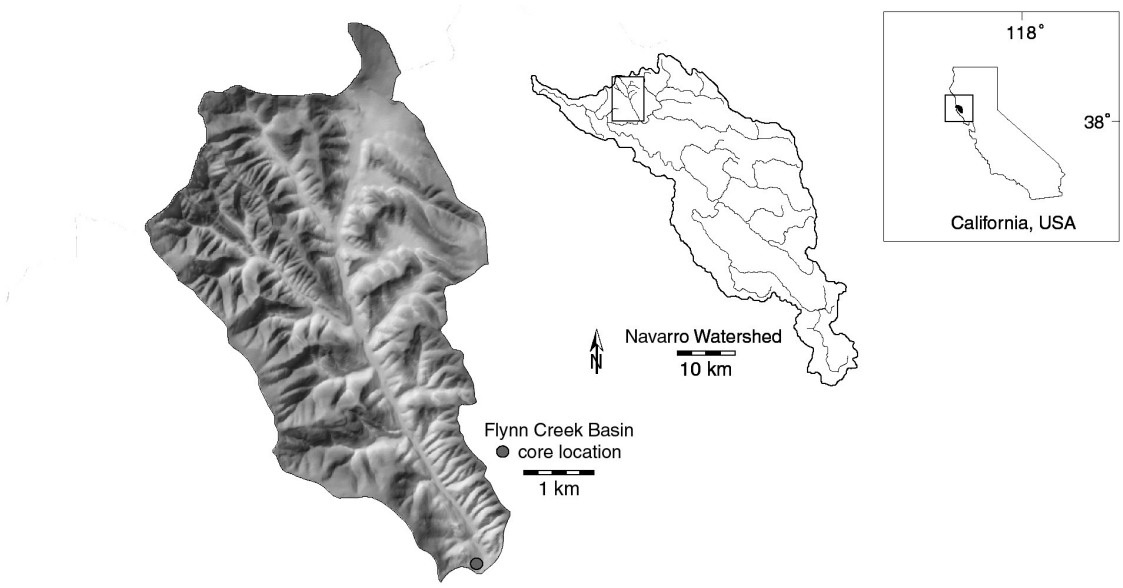

Figure 2-1. Map of Flynn Creek drainage with the location where the core was taken. Topography in the basin is very rugged with an elevation range of 22-358 m. Hillslope gradients range from 0 to 153%. The wetland floodplain from which the core was taken has an area of ~10 m^2. The Navarro watershed drains ~818 km^2 of the Coast Range mountains.

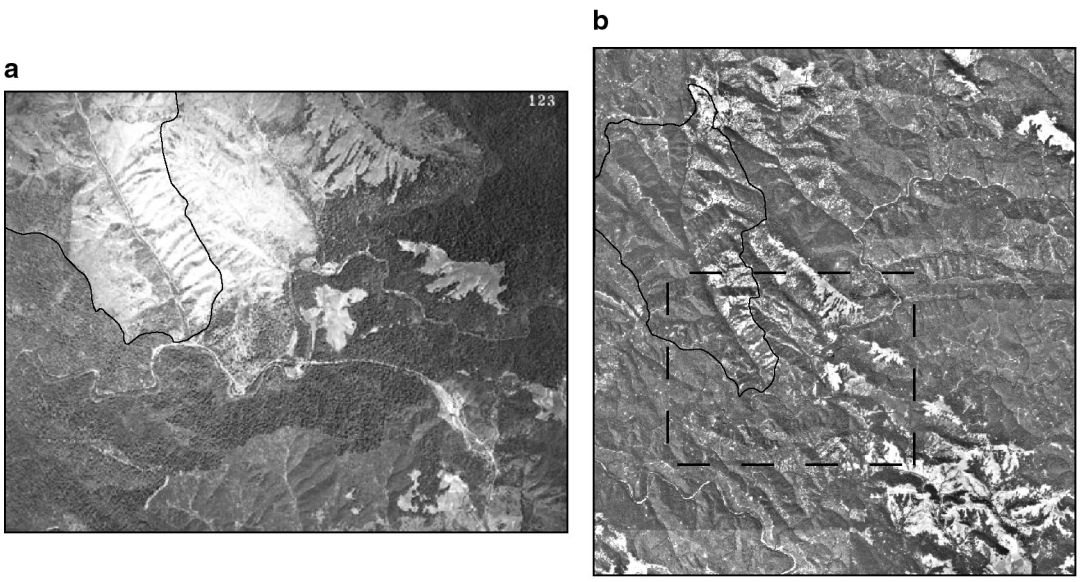

Figure 2-2. (a) Aerial photograph of the lower portion of Flynn Creek basin and surrounding region in 1936 after logging and a fire in 1931 removed much of the forest cover. (b) Satellite image of the basin and region in 1998. The hatched box is the viewing area shown in (a). The outline of the Flynn Creek basin is drawn into both photographs.

Figure 2-3. (a) Overbank deposition rates through time plotted as midpoints; the time-depth model used to construct the time axis is located as an inset. (b) Relative abundance of *Sequoia* pollen through time. (c) Relative abundance of *Alnus* pollen through time. The pollen data show the direct effects of *Sequoia* harvesting in the region and the resulting over-representation or partial replacement by *Alnus*. The hatched lines represent the onset of major anthropogenic disturbances as described in the text.

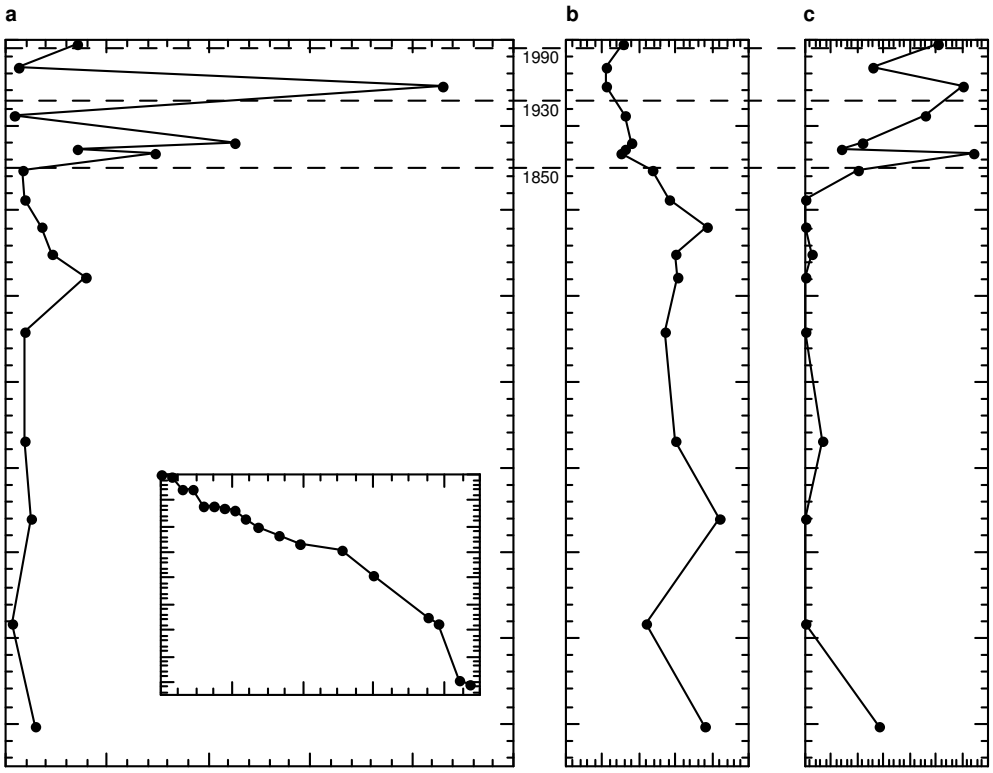

Water temperature

Water temperature is a stressor that poses several problems both in the measurement of the stressor and in understanding its effects on the fish. Numerous studies have been conducted, and numerous reviews are available that document the effects of elevated water temperatures on salmonids. Every species of salmonid has temperature optima established for the various life history stages. And, measurement of water temperature is perhaps one of the simplest and most inexpensive tasks that can be performed. The difficulty of course, comes in establishing stream temperatures along the entire length of the stream system within a watershed, and also to document the temperatures to which fish are exposed. Simply documenting reaches with elevated temperatures is insufficient to establish a negative impact of temperature on the resident salmonids.

In our evaluation of the impacts of temperature on salmonids, we approached the problem in two ways. First, we inserted temperature probes in numerous reaches throughout the watershed including all of the primary stations at which data were collected on fish abundance. We used these data to examine the relationship between various measures of temperature (e.g., maximum, daily range, average daily, average weekly, number of hours with temperatures above an 18^{o}C threshold) and abundance of juvenile salmonids. We then extensively instrumented four pools in 2001, and three pools in 2002 (one pool from 2001 was destroyed due to construction of a bridge over the stream at that location) to determine what was the factor controlling the temperature of water in the pools. During the first year, temperature probes were placed above the water, at 4 depths within the pool, and in the hyporheic zone to measure water temperature at all 6 locations. In 2002, probes were added to water located upstream, in the upstream hyporheic zone, and to the upstream

air. Because pools are particularly critical to the survival of juvenile salmonids during the late summer and fall, understanding the factors that contribute to the reduction of water temperature is important to maintaining a healthy population of juveniles. We examined these data using time series analysis to determine which of the time series appeared to be driving the remaining series'. Data are presented here only for the analysis of the 2001 data.

Finally, because water temperature is extremely heterogeneous throughout the watershed, we were interested in developing a surrogate for water temperature that could be used to evaluate current condition, and as a tool to improve the management of salmonids in the watershed. In cooperation with the North Coast Regional Water Quality Control Board, we developed the RipTopo model to measure actual shading along the stream system in the entire watershed. This model could be used with information about the historical condition of the riparian zone in the watershed to determine where there has been the greatest loss/alteration of riparian vegetation and consequently, the greatest potential for locations that contribute to the temperature load of the stream system.

Temperature Transmission Dynamics – Methodology

This analysis was undertaken in an attempt to understand the potential factors contolling water temperature in pools in the North Fork sub-basin. During the later part of the summer and into the fall, flows become reduced or eliminated entirely leaving large pools as the only available habitat for salmonids. Consequently, the temperature of the water in those pools is critical in determining the growth and survival of the fish. Our analysis centered on the question of whether the temperature of the water in the pools was

determined by the air temperatures immediately above the water, by the temperature of the hyporheic water flowing into the pools, or from surface water upstream flowing into the pools (when surface water flows). During the summer of 2001, four pools were instrumented, and three pools were instrumented in 2002 (Figure 2-5). For each location, the following information is available:

x_t : air temperature measured at 30 min. intervals.

- w_t : Hyporheic average temperature (of three sensors when available), measured at 30 min. intervals
- $Z_t = (z_t^1, ..., z_t^4)'$: pool temperature level at different depths, measured at 15 min. intervals.

For each location, the recorded times for each variable are:

Table 2-3: Minutes on the hour for each record

	Air Temp.	**HOBO Temp.**	**Pool Temp.**			
Location	x_t	w_t	z_t^1	z_t^2	z_t^3	z_t^4
Rail Car Bridge	23'; 53'	17'; 47'	00'; 15'; 30'; 45'			
John Smith Confluence	24'; 54'	22'; 52'				
NLNF Pools	24'; 54'	24'; 54'				
North Fork	24': 54'	28'; 58'				

Therefore, it seemed natural to aggregate the data so that it all shares the same time scale, namely, half-hour intervals. In particular, observations for *x* and *w* would be assigned to the closest 00' and 30' of each hour respectively, whereas the observations corresponding to 15' and 45' for *Z* would be ignored. There is little loss of information in ignoring these

observations since the temperature measurements do not tend to fluctuate very much (often times the temperature does not vary for a span of three hours).

The sample of available data for all four locations and all variables goes from 8/17/01 at 0:00 to 9/7/01 at 2:00, a total of 1013 observations at half-hourly intervals. Data for hyporheic temperature averages is generally available from 8/1/01 to 11/9/01, whereas air temperature measurements are available from 8/1/01 to 9/7/01. Because of the limitations on the availability of pool temperature data, we are unable to take advantage of these larger samples, however. Figure 2-4 displays the time series plot of the data.

Figure 2-4 – Time Series Plot of Temperature Data

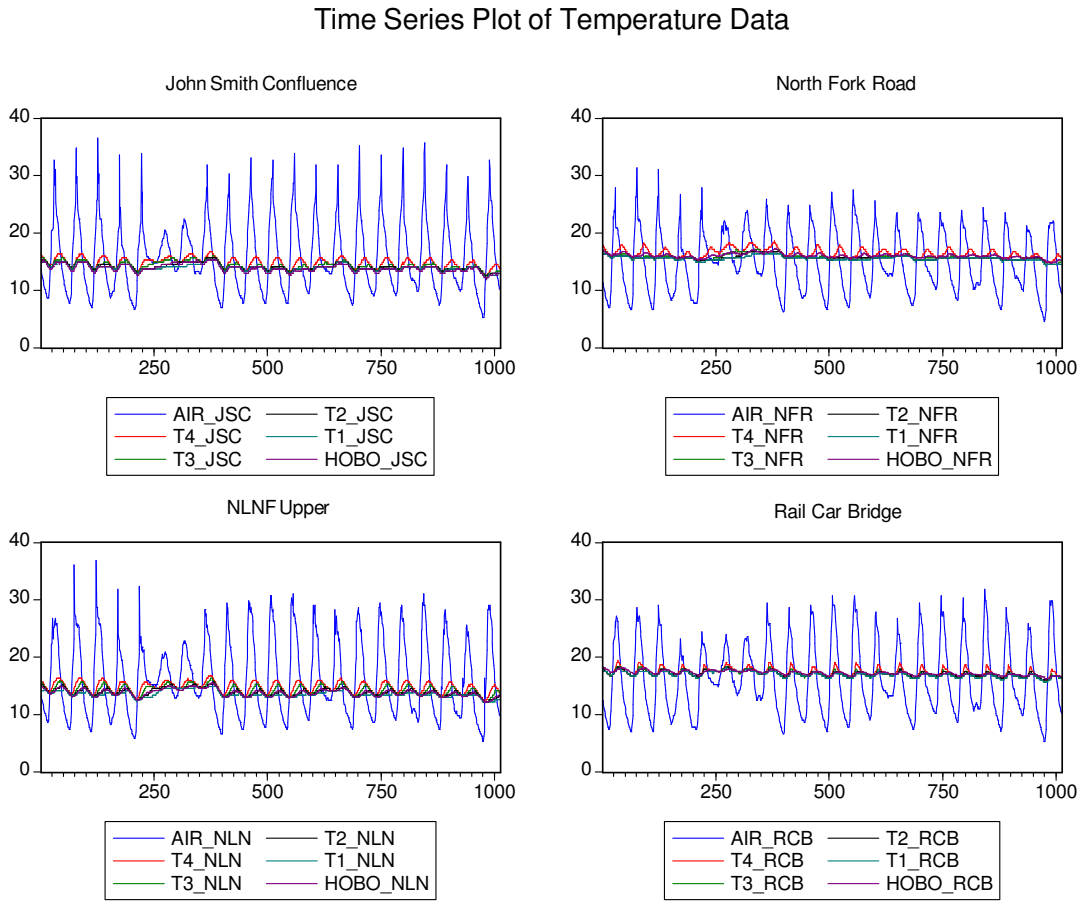

Methodology

The goal of the analysis is to uncover the dynamic response of water temperature to different experiments, usually consisting of 1^0C perturbations. Therefore, let $Y_t = (x_t, w_t, Z_t')'$ collect the available variables, which can be most generally conceived of as a vector of endogenous variables that are jointly determined.

Plots of the data reveal a diurnal seasonal pattern of fluctuations. Although most of the variance in temperatures is determined by these seasonal fluctuations, it is preferable to filter them. At the same time, it is important to preserve the dynamic relations existing between variables, therefore, rather than using more sophisticated spectral-frequency methods (which tend to distort these dynamic relations); it is preferable to use a set of indicator variables. The diurnal seasonal pattern can be captured by a set of 48 binary indicator variables corresponding to each half-hour interval in a day, defined by $d_{jt} = 1$ if observation *t* corresponds to the j^{th} interval of the day; 0 otherwise.

With these considerations in mind, the most natural and general structure describing the dynamic process for Y_t is as a linear system given by the following expression:

$$B_0 Y_t = \sum_{j=1}^{48} \alpha' d_{jt} + B_1 Y_{t-1} + B_2 Y_{t-2} + ... + B_p Y_{t-p} + \varepsilon_t \qquad (1)$$

where α is a vector of coefficients, one for each element in Y_t, that collecs the seasonal effects, *L* is the lag operator such that $LY_t = Y_{t-1}$ and the B_i *i = 1, …, p* are 6×6 coefficient matrices that collect all the coefficients on the lags of Y_t. The standard assumptions on the

error term are $E(\varepsilon_t) = \bar{0};\ E(\varepsilon_t, \varepsilon_t') = D$, D a diagonal matrix. Note that the assumption of diagonality is not restrictive since by design, B_0 captures any contemporaneous correlations between the elements of Y_t.

The system on expression (1) is not usually directly estimable unless one is willing to impose rather severe restrictions on B_0. Rather, the equivalent reduced form model is typically estimated instead,

$$Y_t = \sum_{j=1}^{48} c_j d_{jt} + \varphi_1 Y_{t-1} + ... + \varphi_p Y_{t-p} + u_t \qquad (2)$$

where $c_j = B_0^{-1}\alpha_j;\ \varphi_i = B_0^{-1}B_i; u_t = B_0^{-1}\varepsilon_t; E(u_t) = 0;$ and $E(u_t u_t') = \Omega$. The system in expression (2) is fully identified. The representation in expression (2) is called a *vector autoregression* (or VAR) and is commonly used in practice when one wants to impose minimal restrictions on the data yet obtain meaningful information on its dynamic intercorrelations. Each VAR(p) (where *p* indicates the truncation lag), has an infinite *moving average* representation

$$Y_t = \mu_t + u_t + \psi_1 u_{t-1} + \psi_2 u_{t-2} + ... \qquad (3)$$

where μ_t collects the binary indicator-based mean terms and the ψ_i, *i = 1, 2, …* are 6×6 matrices of coefficients that have the interpretation

$$\frac{\partial Y_{t+s}}{\partial u_t'} = \psi_s \qquad (4)$$

The function that describes this partial derivative is usually called the *impulse response function* and is an example of the type of quantity one may be interested in computing. However, instead we are generally interested in computing

$$\frac{\partial Y_{t+s}}{\partial \varepsilon_{kt}} = \frac{\partial Y_{t+s}}{\partial u_{1t}} \frac{\partial u_{1t}}{\partial \varepsilon_{kt}} + \ldots + \frac{\partial Y_{t+s}}{\partial u_{kt}} \frac{\partial u_{kt}}{\partial \varepsilon_{kt}} + \ldots + \frac{\partial Y_{t+s}}{\partial u_{pt}} \frac{\partial u_{pt}}{\partial \varepsilon_{kt}} \tag{5}$$

where the terms $\frac{\partial u_{it}}{\partial \varepsilon_{kt}}$ can be obtained from realizing that $B_0^{-1}\varepsilon_t = u_t$. Notice that any real, positive symmetric matrix Ω can be uniquely decomposed as $\Omega = ADA'$ where A is a lower triangular matrix with ones in the diagonal, also called the Cholesky factor, and D is a diagonal matrix with positive entries. This realization has led to the common practice of uncovering the structure implied by expression (1) by estimating a reduced-form system as in expression (2) and then imposing some hierarchical ordering on the manner the variables Y_t are contemporaneously intercorrelated. Specifically, given an arbitrary ordering of the elements of Y_t, the Cholesky factorization implies that y_{1t} contemporaneously determines all the remaining variables in the system but is itself independent of them, y_{2t} determines all remaining variables except y_{1t}, and so forth. While there are as many Cholesky factors as possible orderings of the elements of Y_t, the current application contains a natural hierarchy that is related to the view that air temperature is the principal determinant, followed by hyporheic temperatures and then the temperatures of the pools at different depths.

Another interpretation of expression (5) is in terms of forecasts, specifically

$$\frac{\partial Y_{t+s}}{\partial \varepsilon_{kt}} = E(Y_{t+s} \mid y_{kt} = y_{kt-1} + \varepsilon_{kt}; Y_{t-1}) - E(Y_{t+s} \mid Y_{t-1}) \tag{6}$$

Experiments

Expression (6) makes clear the mechanics of the experiment consisting in shocking variable *k* for one period only, and then propagating this shock through the system to observe how other variables in the system are dynamically perturbed. As an example, Figure 2-5 displays this type of exercise for the John Smith Confluence. The left panel of the top row shows how the shock to air temperature declines over time, so that after approximately 7 hours, air temperature returns to normal. On impact, the temperature shock has virtually no effect. However, as time goes by, the maximum effect is felt between 5 to 15 hours after (depending on depth), for a maximum effect of approximately 5% of the original shock.

Figure 2-5 – Impulse responses to a 0.7^0 C one-time shock to air temperature.

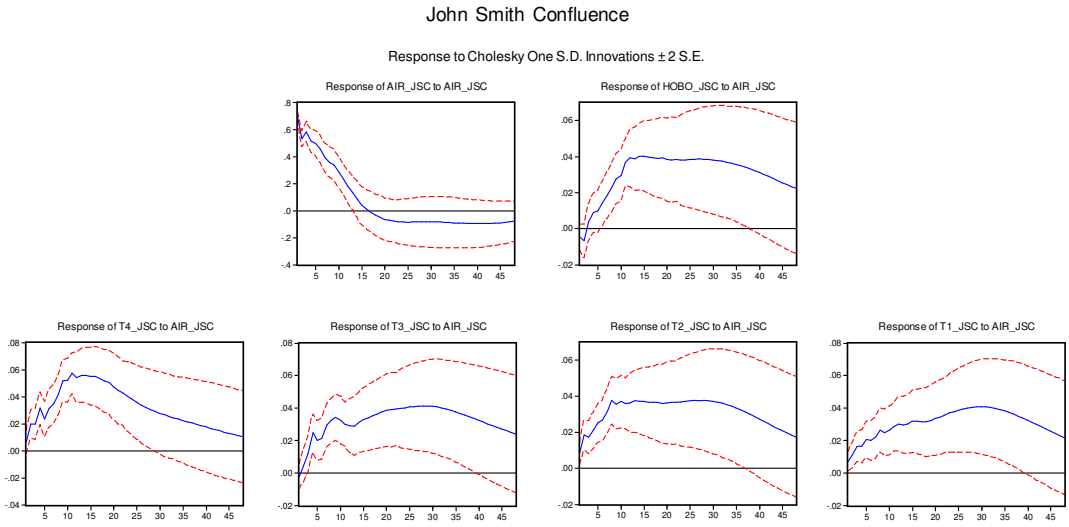

Note: Dotted lines are two standard error bands.

Naturally, it may be more appealing to experiment with other types of scenarios. For example, instead of a one-time shock, one could analyze instead a 1^0 C shock that lasts for

8 hours. This type of experiment can be easily calculated, an example is reported below in Figure 2-6.

Figure 2-6 – Shock lasts eight hours and returns air temperature to baseline.

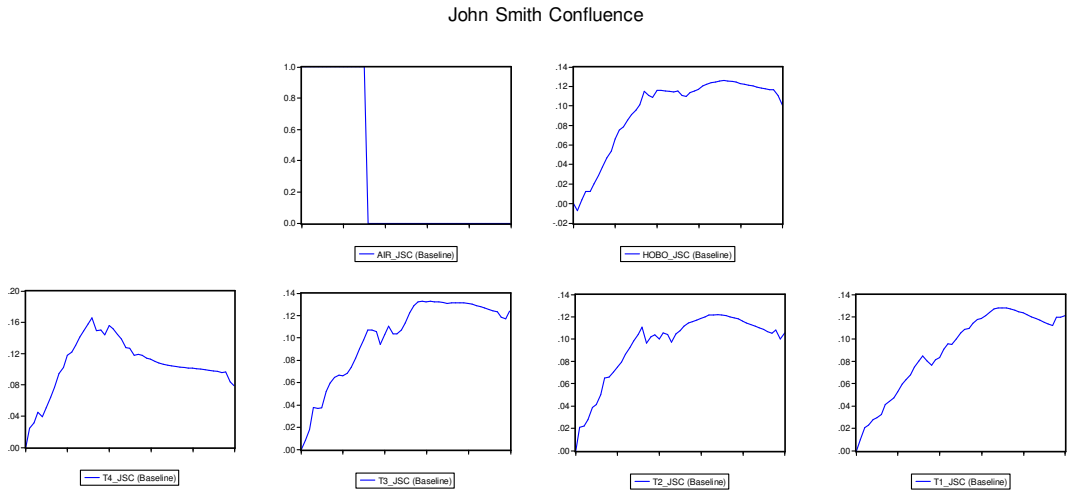

The results indicate that changing the air temperature by 1°C only results in a change in water temperature of about 0.05°C, a very slight change. Our analysis was performed for an increase in temperature, but the results are symmetrical and a similar decline in air temperature would result in a similar decline in water temperature. Consequently, to reduce the temperature of the water approximately 1°C, a decrease in air temperature of 20°C would be required. Such a decrease in air temperature would not be possible simply by improving riparian shading at that site alone. This reduction in temperature would be the reduction required in the air temperature immediately above the pool and does not take into account the possibility of upstream sources. To determine if the upstream sources are critical in determining water temperature, we instrumented the pools in the summer of 2002 to obtain the necessary measurements. Those data are still being analyzed. However, our results do indicate that once heated, it is very difficult to reduce the temperature of the

water in the pools. Hyporheic water, which is traditionally thought to be cooler than surface water was actually warmer in our pools. This is most probably a result of the large amount of hyporheic space and the exchange of surface and hyporheic flows. As the very shallow water flows at the surface, heating would occur as the water passes over large cobbles exposed to the sun. The water is heated to a significant degree and retains that heat as it moves downstream. Another question that arises is where in the upstream section of the watershed does the water receive the largest temperature load. It is possible that the lack of riparian shading upstream leaves sections of the stream open to heating. However, upstream riparian coverage in the North Fork is generally good and there would be few opportunities for a large amount of heat to enter the system. It is also possible that the shallow ground water flows in the watershed are heated as they move downslope prior to entering the stream and that the heat is gained over the landscape. Most probably, a combination of these two explanations is correct. Consequently, we will initiate an analysis of the role of landscape features in determining temperature loading using data obtained over the last two years (see GIS section below). These analyses should be completed during the spring of 2003.

Development of the RipTopo Model of Stream Shading

The Information Center for the Environment at the University of California, Davis, in collaboration with the North Coast Regional Water Quality Control Board, is using a geographic information system to provide applied decision support for watershed management. Our procedure allows for riparian vegetation delineation, quantitative descriptions of land use change, and the identification of key salmonid habitats. The GIS decision support system includes the integration of historical aerial photographs and remotely sensed imagery to provide for the analysis of land use change and current conditions of riparian vegetation. The changes in riparian plant community composition, structure, and extent are an integral element of future watershed management. Analysis at the watershed scale, as performed in our research, allows for a synoptic assessment of mitigative measures and areas of further research. As resource management agencies develop TMDLs for other watersheds, the results and methods used in this study will be of great utility.

The goal of our research is to provide insight into how land use changes influence aquatic and riparian habitats and how these factors relate to salmonid population declines. The following analyses are part of a multi-tiered effort at better understanding the Navarro River watershed at different spatial and temporal scales.

Methods

The Timberland Task Force (TTF) Klamath Province habitat database developed as part of the Klamath Region Vegetation Mapping Project was the primary source of distributed (watershed-scale) vegetation information. Particularly useful database fields included the

vegetation classification by Wildlife Habitat Relationships (WHR) type, tree size classes (classified into diameter at breast height (dbh) ranges), and estimates of percent conifer/percent hardwood for each polygon mapped in the coverage. A polygon is a closed shape defining an area of similar characteristics. To describe potential vegetation height conditions, the mature tree heights for hardwoods and conifers by vegetation class (WHR type) were combined with the polygon percent conifer and percent hardwood values to calculate polygon-specific heights (Table 2-4). For current vegetation conditions, an additional step was performed. Each polygon in the GIS coverage has an associated dbh class. Using a dbh class conversion table, dbh information was converted to vegetation heights for each polygon. Vegetation extent near streams was handled differently for potential and current conditions. For this analysis, all drainages shown on USGS topographical coverages as blueline streams were included in the analysis. The underlying stream network was developed from USGS topographic data, available as a 10m Digital Elevation Model (DEM) coverage. The 10m DEM generated streams coverage is generally close to the USGS blueline streams. Exceptions include areas of low slope and some areas near drainage headwaters. The lateral extent of the 10m DEM coverage used in the analysis was limited to the extent of the USGS blueline streams. For potential conditions, the unvegetated channel was defined using bankfull width, centered on the centerline of the stream channel. Bankfull widths were assigned using a relationship for the Mendocino Coast developed with techniques and equations described in Leopold, Wolman and Miller (1964) and stream channel geometry information (hydraulic geometry exponents needed for the equations) for Mendocino Coast streams developed by Leopold (pers. comm., March 2000). For the current conditions riparian canopy coverage, 1996 aerial

photographs were reviewed and compared to current USGS topographic coverages to determine the occurrence of trees and forested areas in the watershed. The existing riparian vegetation was then digitized on-screen. The analyses were limited to areas within 200 meters of the USGS blue line streams.

Below is a diagram (Figure 2-7) showing the basis of the stream-shading model. A general hillslope (a.) can be characterized by a Digital Elevation Model (DEM); in our model we used a DEM with a 10meter cell size resolution and indicated in the diagram (b.). We then added tree heights (c.) derived from the Mendocino Timberland Taskforce (TTF) forest inventory to the DEM while masking out stream reaches. We employed a standard shading algorithm that calculates the percent incoming solar radiation for each hour (d.) on a given date. Lastly, we summed the hourly values for each reach (e.). One minus the summed percent incoming solar radiation is the stream shade potential.

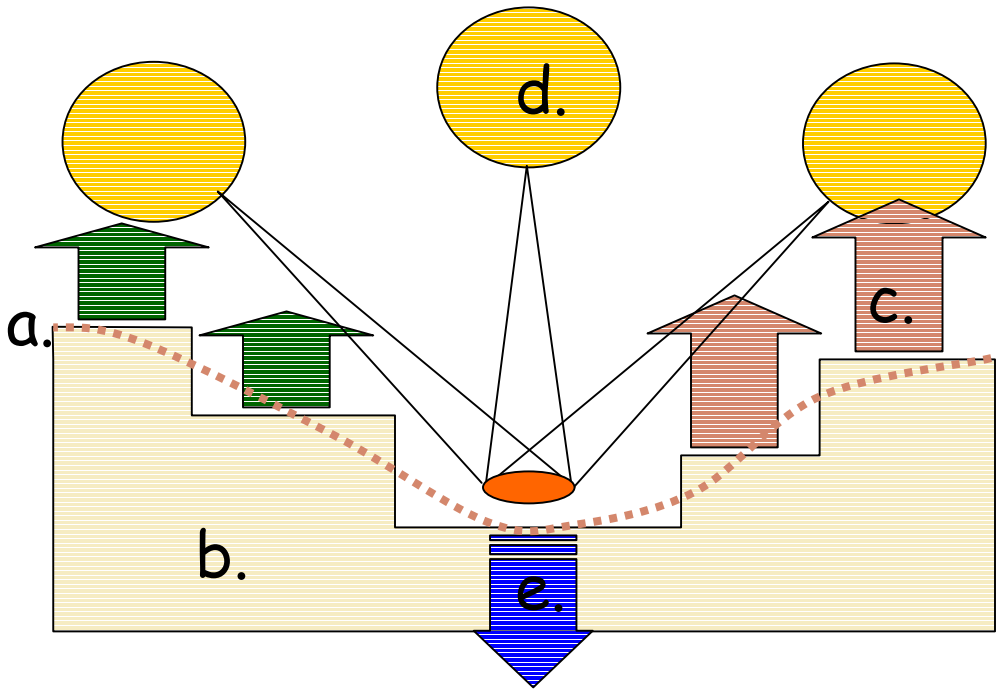

Figure 2-7.

We validated the model using field measurements. We collected riparian species composition and structure data for 90 10m x 10m quadrats located throughout the watershed at fifteen sites. In a comparison of TTF estimated tree heights to measured tree heights on a site-by-site basis, a linear regression indicated that the modeled tree heights and the measured tree heights were similar as indicated in Figure 2-8.

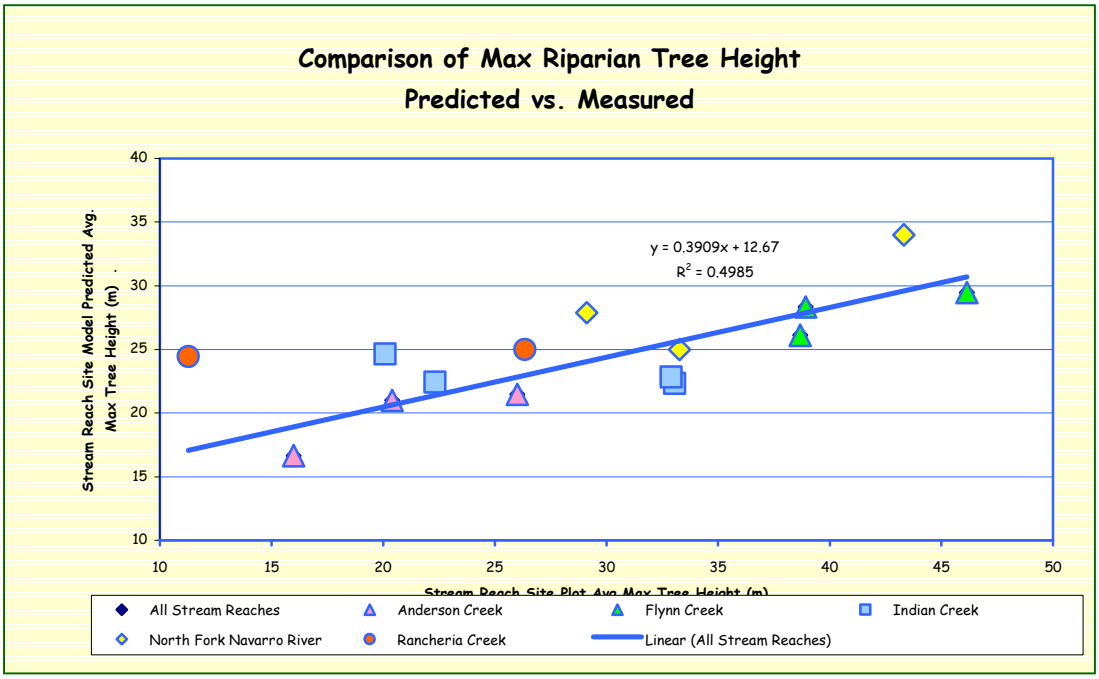

Figure 2-8.

To calibrate the model, the modeled tree heights were used to predict tree heights on the ground with two other variables: elevation and percent slope.

Summary of Fit	
Rsquare	0.813554
Rsquare Adj	0.75762
Root Mean Square Error	5.374183
Mean of Response	29.03812
Observations (or Sum Wgts)	14

Analysis of Variance

Source	DF	Sum of Squares	Mean Square	F Ratio
Model	3	1260.2539	420.085	14.5449
Error	10	288.8184	28.882	Prob > F
C. Total	13	1549.0724		0.0006

Parameter Estimates

Term	Estimate	Std Error	t Ratio	Prob>|t|
Intercept	19.139009	8.49987	2.25	0.0480
Mean(elevation)	-0.076615	0.02049	-3.74	0.0039
Mean(slope)	0.3588636	0.211454	1.70	0.1205
Mean(nvgcc_MEAN)	0.5177788	0.321373	1.61	0.1382

Effect Tests

Source	Nparm	DF	Sum of Squares	F Ratio	Prob > F
Mean(elevation)	1	1	403.81163	13.9815	0.0039
Mean(slope)	1	1	83.18633	2.8802	0.1205
Mean(nvgcc_MEAN)	1	1	74.97109	2.5958	0.1382

Results

First, we tested stream reach plot tree height measurements against stream reach random tree height measurements to determine whether or not the reach could be characterized by our sampling methodology. Based on our preliminary statistical analyses, we had statistically significant results (R^2=0.5887, p=.0.0005) for canopy heights, as defined in the model, and are able to determine that the average height for sampling plots and randomly measured trees along a reach are statistically similar.

Next, we compared the maximum predicted tree heights from the model with the maximum plot tree heights. The results from these analyses were also statistically significant (R^2=0.4985, p=0.0022). Therefore, our model is indicative of the watershed and we can

infer that the sampling plots are statistically similar when compared against the model's predicted values. The initial values from our analyses will be used to calibrate the watershed model. Additional calibration of the model will require further field work efforts.

In addition to fieldwork, we incorporated high-resolution, hyperspectral data generated from AVIRIS (Airborne Visible Infra Red Imaging Spectrometer) into analysis of the watershed. The AVIRIS data collection instrument contains an optical sensor capable of detecting 224 contiguous spectral channels at a resolution of approximately 5m pixels (AVIRIS website). Using a large area, high spatial resolution collection of AVIRIS data for the Navarro River watershed, a classification of riparian vegetation was initiated using a combination of traditional ecological assessment techniques and hyperspectral data analysis. The Navarro River watershed is the focal point of many ongoing, multidisciplinary investigations concerning anthropogenic disturbance of watershed processes, such as logging, road building, and land conversion to vineyards and other agriculture, and resulting ecological responses. Namely, these studies have focused on the role that land use activities play in perturbing anadromous salmonid populations and habitat. Riparian vegetation is a key habitat parameter in that it regulates many of the ecosystem components necessary for salmon reproduction, rearing, and migration through its effect on stream shading, contribution of large woody debris, and allocthonous inputs to the stream system. Thus the identification and assessment of riparian vegetation using hyperspectral analytical techniques is the primary goal of this project; furthermore, it was the intent of the project to use ecological field data to 1) provide a priori expectations of

vegetation classifications, 2) serve as a verification for spectral classification, and 3) to serve as a basis from which to nest the classification results within ongoing, national efforts of cataloging vegetation.

A series of traditional vegetation classification methods were employed on field data to determine the expected species composition of vegetation communities within the riparian zone. The traditional methods of vegetation classification from field collections are based on clustering algorithms and factor analyses, such as TWINSPAN (Hill 1979), and these methods were used to establish an expected distribution of species for the watershed. To aid in the spectral feature extraction, a riparian zone was delineated, to constrain the riparian designation, by using topographic features generated from a digital elevation model of the watershed. The process results in a hierarchical framework with expected species distributions that represent field conditions; this framework was then integrated with hyperspectral feature extraction methods, such as endmember selection, to discriminate different vegetation communities within the riparian zone.

Methods

The following software packages were necessary for the procedures detailed below: ESRI ArcInfo v. 8.0.2; ERDAS Imagine v. 8.5; RSI ENVI v. 3.5; RSI IDL v. 5.5, PARGE v. 1.3 and ATCOR4 v. 2.0, and PC ORD v 4.14.

In all, NASA flew 26 of the 29 proposed flightlines over a period of four days in late July of 2000. For this preliminary hybrid classification analysis, we have chosen 1 representative flightline from the collection to process: FL 17 (Figure 2-9). Elevation of the

study site ranges from sea level to 1054m with most ridge tops paralleling the San Andreas Fault in a southeast to northwest direction toward the Pacific Ocean.

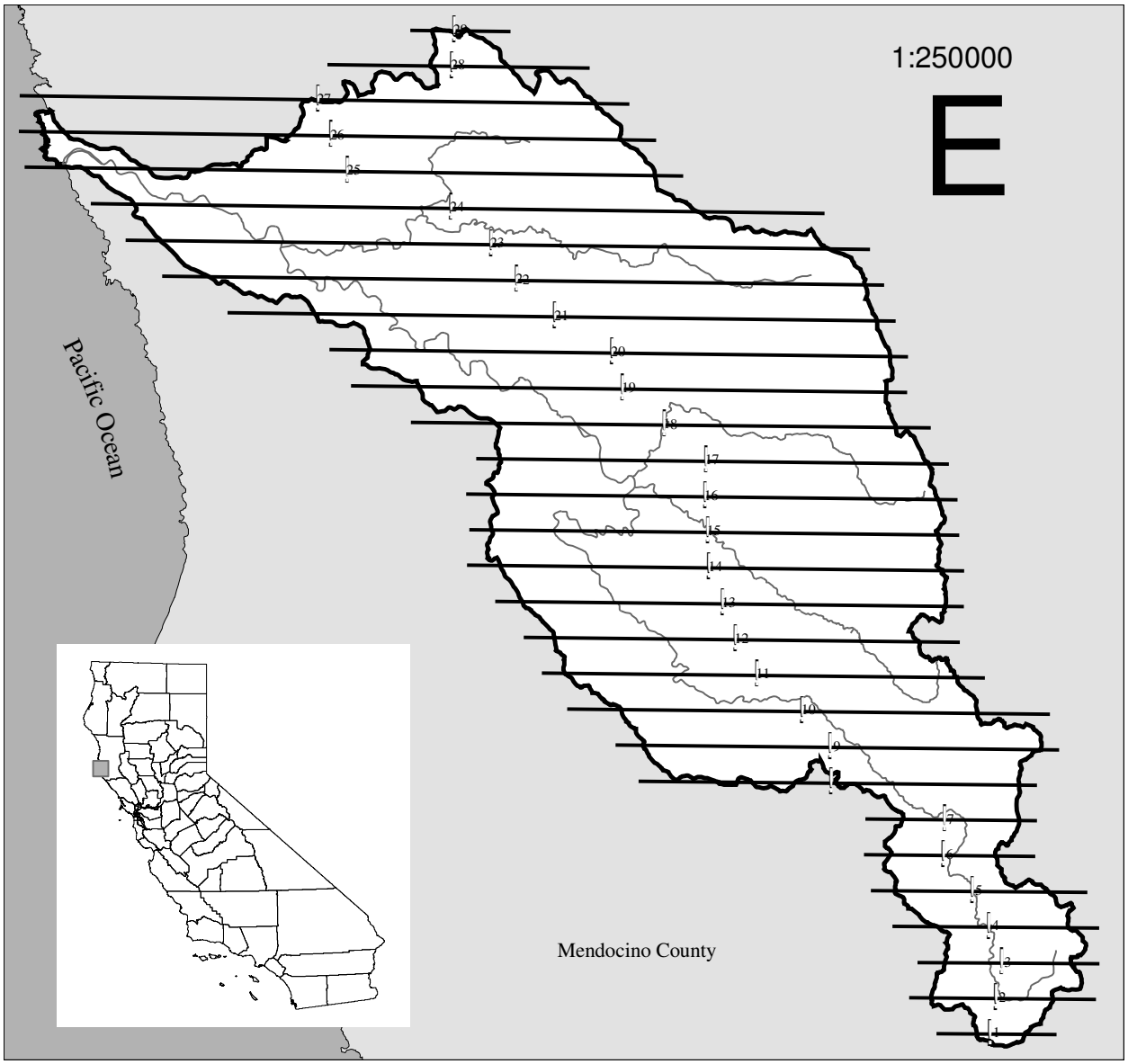

Figure 2-9. Map of the Navarro River Watershed with the proposed AVIRIS flightlines and primary hydrographic features. All but flightlines 1-3 were flown in July 2000. Flightline 17 is the focus of this study. Inset Map shows position of watershed in Mendocino County, California.

AVIRIS data were obtained from NASA Jet Propulsion Laboratory in uncorrected format on 8mm tape. Tape contents were uncompressed to a common file space on a sixteen-processor SGI Origin 2000 supercomputer; each flightline totals approximately 1.5 – 2.5

Gigabytes. To geometrically correct flightline data, a terrain correction software package, Parametric Geocoding (PARGE) (Schläpfer 2000), was used. PARGE integrates the inertial navigation unit readings, flight GPS positions, and ground control points (GCPs) to correct for pitch, roll, heading, and yaw. This procedure also incorporates a Digital Elevation Model to adjust for topographic effects. Prior to initiating PARGE, each frame was mosaicked in ENVI to create a seamless flightline. AVIRIS data were converted from BIP to BSQ in ENVI. GCPs were collected by using a combination of ENVI and Imagine tool sets and Digital Orthophoto Quarter Quadrangles as a visual anchor. GCPs were systematically eliminated based on their X and Y coordinate offsets until the GCP Residual (RMSE) was less than 5.0 m. A 10m USGS Digital Elevation Model of the watershed was resampled to 5m cell resolution and converted in ArcInfo from a grid to a DEM in USGS format (ESRI). The USGS format DEM was imported into ENVI to be used with PARGE, along with the GCPs. The final AVIRIS data were resampled to 5m from the native 3.3m - 4.2m spatial resolution. The geo-corrected results from PARGE, in addition to field spectra of pseudo-invariant targets, such as Navarro Beach and the Boonville Airport, were incorporated into ATCOR4, an atmospheric correction software package (Richter 2000). ATCOR4 corrects for sun angle, atmospheric moisture and particulates, topography, off-nadir viewing angles, and shadows. Once the FLs were geometrically and atmospherically corrected, "noisy" bands were eliminated. Bands were visually inspected and dropped from the analysis if their respective response signatures for a known material deviated from the expected response. The following bands were determined to be acceptable for further analysis: 2-104, 116-152, 168-220 (384.46nm - 1324.15nm, 1443.79nm - 1802.45nm, 1950.66nm - 2469.24nm respectively) and resulted in a final spectral product.

The process for isolating riparian vegetation relies on a hybrid methodology, which incorporates an intersection of two masks, an ecological field data classification, a field-integrated spectral classification, an ecological field data indicator species analysis, and a final spectral un-mixing of indicator species within classes (Figure 2-10). The dual masking procedure is part terrain analysis and part spectral transformation. The spectral masking involved the transformation of the spectral array into three data planes using the Tasseled Cap transformation (Jackson 1983). A processing script was developed in Interactive Data Language (IDL) to extract data planes via the Tasseled Cap procedure for Soil Brightness, Vegetation Greenness, and Water Saturation (Jackson 1983). The IDL script uses Regions of Interest (ROIs) as inputs for each data plane and the spectral downselected bands are used in the input array. To develop a series of ROIs, each FL was transformed using Boardman and Kruse's (1994) Minimum Noise Fraction (MNF) routine to collapse the input data array into 92 dimensions. ROIs were defined for pixels encoded by the Pure Pixel Index (1000 iterations) (Boardman et al 1995) on the MNF transformed arrays. ROIs, in this case, were selected to represent Soil Brightness, Vegetation Greenness, and Water Saturation. Each FL was then examined for the distribution of values from the 3 Band transform array and each plane was bisected to separate materials based on its modal distribution. Vegetation was determined to have a Greenness array value greater than -55.00.

To reduce spectral variability and errant classification of riparian vegetation in upland vegetation communities, the vegetation pixels were further segmented with a Riparian

Extent Mask. The Riparian Extent data grid was created as a combination of two inputs. The first input is a Euclidean distance from streams data grid that was log transformed and rescaled from 1-100. A break point of 37.4 was chosen; it represents one standard deviation less than the mean. The second input represents the least cost path away from streams where Degree Slope is the cost. The results were natural log transformed and rescaled 1-100. A break point of 76.6 was chosen; it represents one standard deviation less than the mean. The Riparian Extent Mask represents the intersection of these two

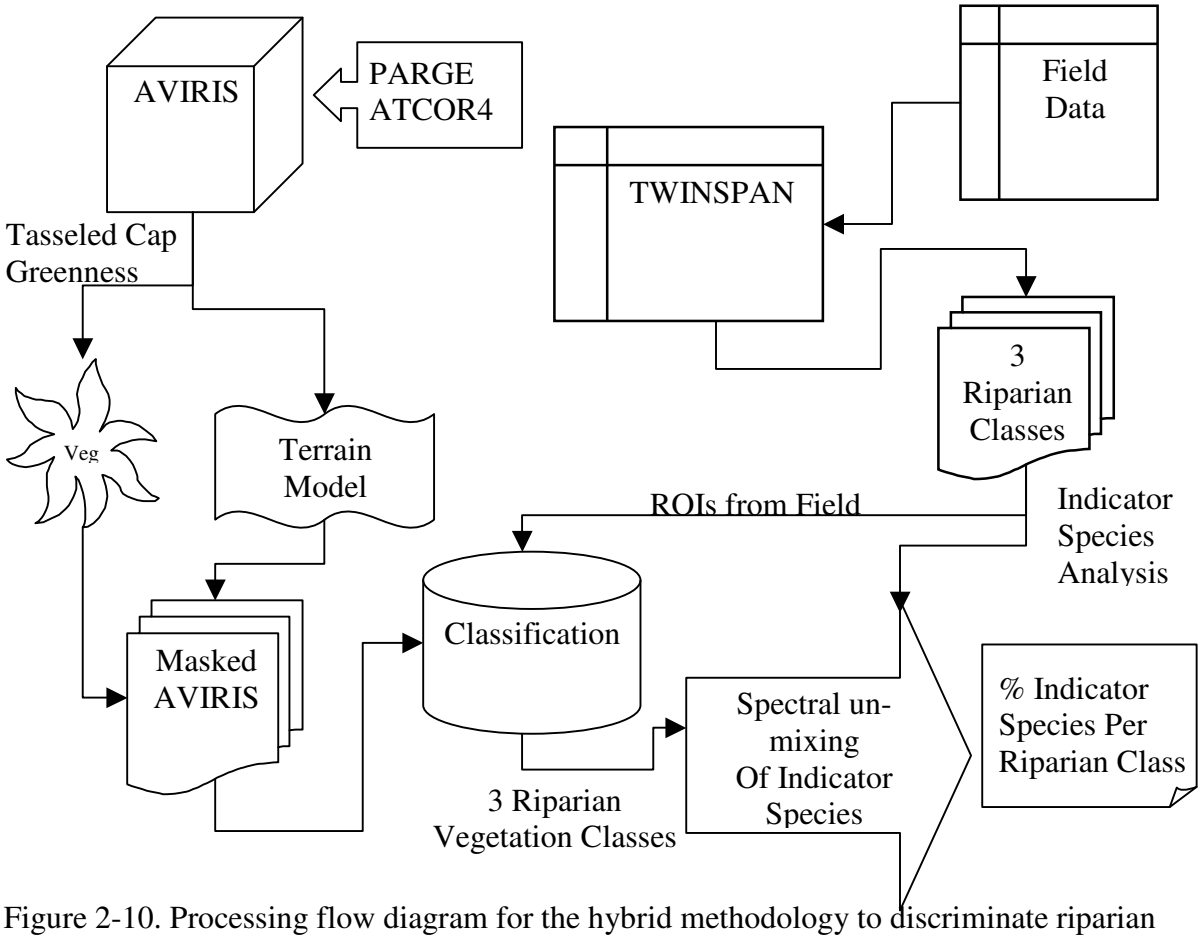

Figure 2-10. Processing flow diagram for the hybrid methodology to discriminate riparian vegetation.

grids. This Riparian Extent Mask was then used to limit the influence of upslope

vegetation on the spectral classification of the AVIRIS data and the Tasseled Cap Greenness plane was used as a mask to restrict the spectral classification to vegetation solely. The supervised classification incorporated the results of ecological data analysis of fieldwork conducted in the summer of 2000. The riparian fieldwork consisted of 6 - 10m x 10m quadrats randomly placed along each Study Reach at 16 Study Sites throughout the watershed. Study Sites were stratified to represent major tributaries in the watershed and position in the watershed, in terms of upstream accumulative drainage area. Ultimately, this stratification also recognizes differences in elevation; different geologic substrates; and distance to the Pacific Ocean, a primary climatological determinate. We identified all woody species, estimated percent cover of each woody species, measured all stems > 10cm DBH, measured tree heights with a LaserTech Impulse 200 Rangefinder, and located quadrat boundaries with a Trimble ProXRS DGPS. The species cover data were analyzed using Two-Way Indicator Species Analysis (Hill 1979, McCune and Mefford 1999). TWINSPAN can be described as dichotomized ordination analysis, in that an iterative character weighting is used to separate species affinities based on the incorporation of *pseudo-species* to represent differences in abundance for each observed species (van Tongeren 1995). Similarly, sample sites are dichotomized and, ultimately, added to a species-by-site matrix. The result of this ordination is a fidelity matrix with an approximate positive diagonal, from upper-left to lower-right, which can be used to characterize un-sampled sites (van Tongeren 1995); in this exercise, it is used as an *a priori* guide to vegetation communities within the riparian zone and resulted in three broad classes (Appendix 2-1). Lastly, in terms of the ecological field data analysis, an Indicator Species Analysis was performed using the three Riparian Vegetation classes derived from

TWINSPAN (Dufrene and Legendre 1997). Indicator Species Analysis is a method that combines information on the concentration of species abundance for a particular group and the faithfulness of occurrence of a species in that group, as a function of frequency (McCune and Mefford 1999). It produces indicator values for each species in each group, reflecting abundance and frequency, and this score is tested for statistical significance using a Monte Carlo technique (McCune and Mefford 1999).

A parallelepiped classification was performed in ENVI using ROIs defined by the field quadrat boundaries, and coded to represent the TWINSPAN classification. To estimate the percent indicator species composition for a particular class, the Spectral Angle Mapper classification (Kruse et al 1993) was performed in ENVI on the masked AVIRIS vegetation data using endmembers from the Jasper Ridge spectral libraries for coast redwood, California bay laurel, and arroyo willow with a 0.1 radian deviance threshold from the library spectra for classification.

Results

Using minimum criteria for TWINSPAN classification of field data, three broad classes of vegetation emerged. Two classes are typically considered upland vegetation; however, they are well represented in the riparian zone (Class A & B). These two classes have three species that are ubiquitous and representative: California bay laurel (*Umbellularia californica*), Douglas-fir (*Pseudotsuga menziesii*), and tanoak (*Lithocarpus densiflorus*). These two classes are separated by two diagnostic species: coast redwood (*Sequoia sempervirens*), and big-leaf maple (*Acer macrophyllum*); representing wetter and drier climes respectively. Other species that are marginally diagnostic are Pacific madrone

(*Arbutus menziesii*) for wetter environments and coast live oak (*Quercus agrifolia*) for drier environments. The riparian class (Class C) is represented by a heterogeneous mixture of species; however, arroyo willow (*Salix lasiolepis*), Himalayan blackberry (*Rubus discolor*), and white alder (*Alnus rhombifolia*) emerged as diagnostic species. Other indicator species in this riparian class are: California blackberry (*Rubus vitifolius*), Pacific dogwood (*Cornus nuttallii*), and white willow (*Salix alba*). Furthermore, many of these species have significant Indicator Values in determining riparian class (Table 2-4, at end) as determined by Indicator Species Analysis, which determines a species Indicator Value as a function of abundance and frequency (Dufrene and Legendre 1997). For Class A, redwood had the highest Indicator Value. For Class B, California bay laurel was the best indicator species. And lastly, arroyo willow has the highest Indicator Value for Class C.

The results of the parallelepiped classification were an overall accuracy of 77.8% and a Kappa coefficient of 0.6814. These results suggest that the three riparian classes were well represented in the classified image and that the input ROIs, representing the TWINSPAN classification of the field data, are indeed different communities and that these vegetation communities vary spectrally. The results of the Spectral Angle Mapper classification for the three Indicator Species (Table 2-5), derived from the Indicator Species Analysis, are poor in describing the vegetation community class as a function of Indicator Species presence. This is evidenced by the fact that only California bay laurel (*Umbellularia californica*) was the only Indicator Species to predominate its Riparian Vegetation Class by percent of pixels within class. However, these results are preliminary and could change with the incorporation of other flightlines and other field plots. Some reasons for the current results are: 1) the mixed composition of vegetation communities are difficult to

separate spectrally by species; 2) vegetation spectra from libraries are not ideal for isolating those same species under different field conditions; or 3) using spectra as endmembers that are very close in vector space is not an ideal condition.

Class	Indicator Species	No. SAM Pixels	No. Class Pixels	Pct. Indication by SAM
A	**Salix lasiolepis**	50	15508	0.32
B	*Salix lasiolepis*	2151	41163	5.23
C	*Salix lasiolepis*	3543	44461	7.97
A	*Sequoia sempervirens*	165	15508	1.06
B	*Sequoia sempervirens*	6669	41163	16.20
C	*Sequoia sempervirens*	9965	44461	22.41
A	*Umbellularia californica*	0	15508	0.00
B	*Umbellularia californica*	175	41163	0.43
C	*Umbellularia californica*	1833	44461	4.12

Table 2-5. Results of Spectral Angle Mapper Classification on Discriminated Riparian Vegetation using Jasper Ridge Spectral Library for selected Class Indicator Species.

The preliminary results of this effort indicate that hybrid methods of feature extraction work best in this varied landscape of topography, climate, and vegetation communities. Additional research will be focused on assessing other discriminatory methods for feature extraction within the riparian zone and other feature types. However, assessing the distribution and composition of riparian vegetation at a watershed scale is essential to protecting salmonid habitat and guiding restoration efforts. The methods outlined here, as they are improved, will aid land use managers in their ability to inventory, restore, and monitor riparian ecosystems. This is particularly true for north, coastal California watersheds where recent policy determinations under the federal Clean Water Act and

Endangered Species Act require regulatory agencies to assess ecosystem integrity in a comprehensive and timely manner.

Future Products

Description of Streamside Vegetation. We will be developing methods for evaluating riparian vegetation condition along distinctly different geomorphic reaches. This will involve stratifying stream channels as Source, Transport and Depositional reaches; evaluation of the AVIRIS riparian classification by these strata will inform resource managers as to the expected riparian composition in different management units.

Riparian Vegetation Biomass. The evaluation of band combinations, vegetation enhancing spectral transformations, and vegetation indices will be used to estimate relative contributions to forest biomass within a predefined riparian zone (i.e., Riparian Extent Mask or Regulated Buffer Zone). This will include comparison of vegetation indices with field-based measurements of forest structure (canopy height, DBH, percent cover, etc.).

Vegetation Structural Attributes. We will be examining the potential of AVIRIS data to estimate vegetation structural attributes, including canopy cover, size and vertical structure (i.e. single story vs. multi-story). This will include a comparison of estimates with those from USFS vegetation maps and with field measurements. This accuracy assessment of the AVIRIS derived riparian vegetation map will help evaluate how well the AVIRIS classifications compare with the existing USFS vegetation maps in the riparian zone.

Table 2-4. List of taxa used in the indicator analysis.

	Taxon Name	Common Name	Class	Indicator Value	p*
1	*Salix lasiolepis*	arroyo willow	C	53.7	0.001
2	*Acer macrophyllum*	big-leaf maple	B	30.7	0.015
3	*Umbellularia californica*	California bay	B	68.1	0.001
4	*Quercus kelloggii*	California black oak	B	13.2	0.069
5	*Rubus ursinus*	California blackberry	C	20.8	0.121
6	*Aesculus californica*	California buckeye	B	2.4	1
7	*Rhamnus californica*	California coffeeberry	A	10.8	0.109
8	*Corylus cornuta var. californica*	California hazelnut	A	11.9	0.225
9	*Torreya californica*	California nutmeg	B	7.1	0.481
10	*Vitis californica*	California wild grape	B	7.3	0.415
11	*Quercus chrysolepis*	canyon live oak	B	10.5	0.159
12	*Quercus agrifolia*	coast live oak	B	17	0.069
13	*Sequoia sempervirens*	coast redwood	A	83.4	0.001
14	*Ceanothus incanus*	coast whitethorn	B	7.9	0.189
15	*Salix hookeriana*	coastal willow	C	6.6	0.327
16	*Arctostaphylos manzanita*	Common manzanita	B	2.6	1
17	*Baccharis pilularis*	coyote brush	C	14.3	0.023
18	*Pseudotsuga menziesii var. menziesii*	Douglas-fir	A	45.4	0.005
19	*Abies grandis*	grand fir	A	10.7	0.143
20	*Rubus discolor*	Himalayan blackberry	C	70.4	0.001
21	*Arbutus menziesii*	Madrone	A	9	0.587
22	*Fraxinus latifolia*	Oregon ash	B	3.4	0.762
23	*Cornus nuttallii*	Pacific dogwood	C	15.4	0.021
24	*Taxus brevifolia*	Pacific yew	B	5.1	0.579
25	*Toxicodendron diversilobum*	poison oak	B	13.8	0.119
26	*Alnus rubra*	red alder	B	4.7	0.662
27	*Salix laevigata*	red willow	C	7.7	0.139
28	*Rubus spectabilis*	salmon berry	B	5.3	0.498
29	*Salix sessilifolia*	sandbar willow	B	2.6	1
30	*Salix sitchensis*	Sitka willow	C	7.7	0.15
31	*Lithocarpus densiflorus*	Tanoak	A	63.2	0.001
32	*Heteromeles arbutifolia*	Toyon	C	5.1	0.447
33	*Quercus lobata*	valley oak	B	10.5	0.103
34	*Myrica californica*	wax-myrtle	A	5.4	0.311
35	*Rhododendron occidentale*	western azalea	A	15.4	0.038
36	*Plantanus racemosa*	western sycamore	C	7.7	0.135
37	*Alnus rhombifolia*	white alder	C	51	0.001
38	*Salix alba*	white willow	C	23.1	0.006
* proportion of randomized trials with indicator value equal to or exceeding the observed indicator value (Dufrene and Legendre 1997).					
p = (1 + number of runs >= observed)/(1 + number of randomized runs)					

Water quality analysis

Water quality analyses were performed on samples collected during the winters of 1999-2001. Water was collected directly from storm drains from Highway 128, from bridges on Highway 128, and from surface waters. Both inorganic and organic constituents were identified and quantified. Statistical analyses of those data are still in progress. A large database of those values has been constructed and is available upon request. We anticipate that we will finish the data analyses by mid-2003. The only inorganic constituent that was found in relatively high concentrations was zinc, although zinc is a normal constituent of crustal materials and is naturally found in high concentrations in this region. We used zinc as a stressor in dietary exposures of coho salmon to determine if there is an interaction between levels of zinc and high water temperatures common in the watershed (Volume III).

Toxicity

Several samples were collected for toxicological testing at the UC Davis Aquatic Toxicology Laboratory. The standard three species EPA toxicity test procedure was used to estimate the amount of toxicity in the samples. Summer samples were collected as a baseline, but significant toxicity was detected at six locations on July 28, 2000.

Storm water runoff was collected twice in October 2000. No toxicity was detected in samples associated with any runoff event despite the fact that metals were detected in high concentration in runoff directly collected from Highway 128. No samples were collected directly from the storm drains because logistical difficulties in obtaining sufficient volumes of water from storm drains. As indicated by the toxicity test results, receiving waters tested directly downstream from the point of entry of the storm drains were not toxic.

Storm water collected at the end of January 2001 produced significant toxicity in the fathead minnow test, but not in the *Ceriodaphnia* nor *Selanstrum* tests. This indicates that the probable cause of the toxicity is pathogen related, and the TIE was performed to verify the causal agent. Results of the TIE indicate that pathogens are the agent causing mortality in the fathead minnows.

Results of the toxicity tests are in general agreement with the analyses of amounts of metals in fish tissues. Liver and gut material in steelhead were analyzed for concentrations of several metals including arsenic, cadmium, copper, iron, lead, manganese, mercury, molybdenum, and zinc. Some individuals had elevated levels of individual metals such as mercury, lead and arsenic, but the only metal that was consistently elevated was zinc. The

source of the zinc is unknown, but based on the ubiquitous nature of zinc in the watershed, it is assumed that the zinc originates from natural sources and is not anthropogenically generated. An experiment was conducted using hatchery coho salmon to evaluate the interaction between zinc and temperature in causing toxicity. Results indicate that zinc and increased temperatures negatively impacted both fish growth and behavior, but that no statistically significant interaction existed between the two stressors. Consequently, no additional decrease in growth or survival is expected to occur at locations in which fish are exposed to both elevated zinc and increased temperatures.

Biotic Stressors

Interspecific competition between California roach (*Lavinia symmetricus*) and juvenile steelhead trout (*Oncorhynchus mykiss*)

Introduction

In our study, we looked for the effects of interspecific competition from California roach (*Lavinia symmetricus*), a common minnow (Cyprinidae), on young-of-the-year (YOY) steelhead trout in a North Coast stream. Interspecific competition between steelhead trout and different cyprinid species has received much attention from researchers in other regions of the country (e.g. Reeves et al. 1987, Grossman and Boulé 1991, Reese and Harvey 2002). This is primarily due to the fact that fish assemblages containing steelhead trout are often co-dominated with one or two cyprinid species that show considerable resource overlap (Moyle 2002). Although steelhead trout and California roach are similarly distributed along the North Coast, there has been no direct research into the effects of interactions between the two species on steelhead trout populations.

In the Navarro River system (Mendocino Co.), steelhead trout and California roach are frequently two of the most common fishes in a given reach (J. Feliciano, unpublished data).

Juvenile steelhead trout aggressively defend feeding territories against both conspecifics and other fish species (e.g. Hartman 1965, Everest and Chapman 1972, Harvey and Nakamoto 1997, Kelsey et al. 2002). Although California roach are less aggressive (Moyle 2002), numerous field studies provide evidence suggesting that these two species might compete for resources. Fite (1973) found a 40% diet overlap between YOY steelhead trout and California roach from March to October 1972 in the Eel River, a similar Northern California waterway. Also on the Eel, Power (1990) observed that enclosed and free-swimming adult California roach and juvenile steelhead trout ate the same food items. Fite (1973) also reported an overlap in habitat use – YOY steelhead trout were found primarily in riffles and the upstream ends of pools while California roach occupied and fed in all habitat types. In Deer Creek, a tributary to the Sacramento River, Moyle and Baltz (1985) found that YOY steelhead trout and adult California roach showed similarities in preferred focal point water velocity, relative water depth, and substrate type. Taken together, these observations point to the potential for competition to exist between the two species. We conducted a manipulative field experiment to test this hypothesis and increase our understanding of how, when, and where interspecific competition affects steelhead trout populations in the Navarro River system.

We decided to use YOY steelhead trout and adult California roach because the species' diet and habitat use are most similar at these life history stages (Fite 1973, Moyle and Baltz 1985). Juvenile California roach occupy shallower and slower habitats while older juvenile steelhead trout prefer deeper, faster water (Moyle and Baltz 1985). Furthermore, larger juvenile steelhead trout prey upon California roach juveniles and fry (Power 1990, Moyle

2002). Due to the steelhead trout's aggressiveness, we incorporated treatments that let us look for both intraspecific competition among steelhead trout and interspecific competition between steelhead trout and California roach. Such a design would allow us to assess the relevance of any interspecific effects we found.

Methods

Study Site

We conducted the experiment in August and September 2000 in a 2-km stretch of the South Branch of the North Fork Navarro River (Mendocino County, CA). The fish assemblage of the study reach is entirely native, comprising 3 anadromous and 4 freshwater species. The freshwater stages of two of the anadromous species, steelhead trout (*O. mykiss*) and coho salmon (*O. kistuch*) are water column-feeding insectivores (Moyle 2002). The third, Pacific lamprey (*Lampetra tridentata*), is a substrate-dwelling filter feeder while in its larval freshwater stage (Moyle 2002). Two of the freshwater species, prickly and coastrange sculpin (*Cottus asper* and *C. aleuticus*, respectively) are benthic dwelling predators. The remaining two fish species, threespine stickleback (*Gasterosteus aculeatus*) and California roach (*Lavinia symmetricus*), are small omnivores. Threespine stickleback feed primarily from the benthos and aquatic vegetation while California roach feed from both the benthos and water column (Moyle 2002). Steelhead trout and California roach are the most common fish species in the study reach, each comprising approximately 45% of the fish assemblage. Threespine stickleback, Pacific lamprey ammocoetes, and the two sculpin species were less common but were regularly observed during the study and in pre-study surveys (J. Feliciano, unpublished data). Juvenile coho salmon, a federally

endangered species, were very rare, having been observed only once in the study reach during three years of surveys.

The region typically experiences high levels of precipitation, with virtually all of it delivered as rainfall during the October – May wet season (Mount 1995); from 1978 to 2000, mean annual rainfall was 1.24±0.1m (SE) (D. Slota, California Department of Foresty, pers. comm.). Consequently, stream fish in the area are subjected to extremely high flows during the winter and periods of very low flow and severe habitat reduction during the late summer. Areas within the drainage basin have been logged intermittently over the past 50 years, with the most extensive activity occurring in the late 1980s (C. Surfleet, Mendocino Redwood Company, LLC Staff Hydrologist, pers. comm.). Currently, most of the basin is covered by a dense forest dominated by redwood trees (*Sequoia sempervirens*).

Experimental Design

We built 16 13m^2 instream fish enclosures along the study reach at sites that were similar in flow and habitat characteristics. The upstream sides of the enclosures were positioned perpendicular to the flow at the downstream ends of riffles. The walls of the enclosures were constructed from 5mm knotless nylon seine netting attached to 16mm diameter rebar pounded into the streambed. The netting material allowed potential prey items such as macroinvertebrate drift and post-larval fish into the enclosures but prevented YOY steelhead trout or adult California roach movement across the barrier. We sealed the bottoms of the enclosures with sand, gravel, and pebbles taken from the adjacent stream

banks. To exclude terrestrial predators, we suspended monofilament gill netting over the tops of the enclosures.

We varied the enclosures' shapes to account for the irregular conformation of the stream channel and to make the habitat within the enclosures as similar as possible to each other and to the types of habitat available to fish in unmanipulated stream reaches. Mean water depth in each enclosure was 0.27±0.02m and mean maximum water depth was 0.60±0.03m. The mean water temperature over the duration of the experiment was 15.8C with a mean diurnal range of 2.7C. Mean shade over the enclosures was moderate (64±1.5%) and gravel and pebbles dominated the stream bottom. Each enclosure contained areas of flowing and still water (mean volumetric flow = 0.05±0.02m^3/s; mean maximum water velocity = 0.2±0.03m/s). Flowing habitats were defined as areas where the fish swam actively to maintain their position in the water column and generally faced upstream. In still water habitats, the fish did not have to orient themselves and swim upstream to maintain their position relative to the stream bottom. The enclosures contained all of the habitat types available in the study reach except for shallow riffles, very deep (>1m) pools, and undercut banks. Al though these areas can represent important habitat for both steelhead trout and California roach, it was impossible to include these habitat types and ensure that the enclosures remained intact and fish-proof for the duration of the experiment. Furthermore, pre-enclosure fish densities were highest at the upstream ends of pools in the habitat types that were contained within the enclosures.

During pre-experiment surveys, we found that the mean density of fish along the study reach was 1.4 fish/m^2 and that equal proportions of YOY steelhead trout and California roach dominated the fish community. We used these data to determine the treatment combinations for the experiment. We combined YOY steelhead trout and adult California roach into four treatment combinations: 1) 9 steelhead trout and no California roach, creating an enclosure density of 0.7 fish/m^2, 2) 9 steelhead trout and 9 California roach, or 1.4 fish/m^2, 3) 18 steelhead trout and 0 California roach, and 4) 18 steelhead trout and 9 California roach, or 2.1 fish/m^2. These combinations allowed us to test simultaneously for the presence and relative effects of YOY steelhead trout/California roach competition and intraspecific competition among YOY steelhead trout (Connell 1983, Goldberg and Scheiner 1993, Fausch 1998). Using 16 instream enclosures allowed us to have four replicates of each treatment combination. Preliminary analyses indicated that four replicates were needed to achieve 80% power at the $\alpha = 0.05$ level (Zar 1999). To account for potential habitat variation along the study reach, we incorporated a randomized complete block design when assigning the treatments to the enclosures. Each block consisted of four consecutive enclosures.

We used beach seines, minnow traps, and electrofishers to capture fish for the experiment. Mean initial steelhead trout standard length and mass were 54.22 ± 0.64mm and 2.76 ± 0.10g, respectively. Mean initial California roach standard length and mass were 56.33 ± 1.15mm and 4.12 ± 0.33g. As much as possible, we chose fish that reflected the natural size distribution within the stream. However, both the size of the enclosure netting and design of the fish marking system created a lower size limit of approximately 45mm

standard length for both species. Each steelhead used in the experiment was anesthetized with a clove oil solution (Anderson et al. 1997), measured, weighed, and given a unique fin tattoo (MicroJect 100, NewWest Technologies). Since California roach did not respond well to anesthetization and prolonged handling, we only measured and weighed them before placing them in their assigned enclosures. After a 24-hour acclimation period, we snorkeled the enclosures to check on the health of the fish and replace any fish that died from handling. We returned to the enclosures every second or third day to remove debris that had collected on the enclosure walls. The fish were allowed to grow in the enclosures for six weeks.

Fish behavior in each of the enclosures was monitored during two morning and two evening observation periods spread out over three days in the fourth week of the experiment. Snorkelers observed randomly selected fish from outside of the netting and verbally reported fish activity to a recorder on the shore. Three 3-minute observation periods were tallied for each species present in each enclosure – a total of 576 observation minutes for steelhead trout and 288 observation minutes for California roach. The snorkeler reported feeding activity observed in the water column or on the benthos, and intra- and interspecific attacks received. The habitat type, either flowing or still water, occupied by the fish was also recorded. From these data, we calculated feeding rate and intra- and inter-specific attack rate, feeding location, and habitat use.

At the end of the experiment, we removed and weighed all of the fish used. We calculated mean change in mass per steelhead trout for each enclosure. We preserved the fish in a

10% Formalin solution and then dissected out their stomach or foregut contents to compare diets. We divided the contents into vegetation, animal, and unidentifiable portions, identified the animal contents to lowest taxonomic level, and then dried them separately for 24 hours in an oven held at 55C. After drying, we calculated total diet mass and the proportions, by mass, of animal or plant material. To assess the effects of the enclosures on the growth and diet composition of the experimental fish, we also collected and dissected YOY steelhead trout and adult California roach from outside of the enclosures at the end of the experiment.

Data Analysis

We defined YOY steelhead growth as the mean change in mass per fish per enclosure. To conform with the assumption of normality, we used a ln(Y+1) transformation prior to the statistical analyses. We used the transformed growth and diet mass data as the response variables in two separate two-factor ANOVAs. The two independent factors were the same for both ANOVAs - initial steelhead trout density and California roach presence/absence.

To analyze the fish behavioral data, we used a series of repeated measures ANOVAs based on a general linear model. We used the behaviors from the four separate observation bouts per enclosure as the within-subjects factors and fish species, habitat type (i.e. flowing or non-flowing) and treatment combination as the between-subjects factors. The dependent variables were steelhead trout and California roach attack rates, and water column and benthic feeding. We used a separate RM ANOVA to assess differences is habitat use - percent time spent in riffles was the dependent variable while treatment combination and

species were the independent variables. When appropriate, we incorporated a sequential Bonferroni test to adjust the alpha levels for each test when appropriate (Rice 1989).

Results

Steelhead trout in the low-steelhead-density enclosures gained an average of 3.5 times more mass than steelhead in the high-steelhead-density enclosures. The presence or absence of California roach had no effect on steelhead trout growth (Figure 2-11). In the low steelhead density enclosures, steelhead trout gained an average of 1.02 ± 0.31g when California roach were present and 1.18 ± 0.53g when they were absent. In the high steelhead density enclosures, mean steelhead mass gain was 0.31 ± 0.11g in the presence of California roach and 0.26 ± 0.10g when they were absent. Mean survivorship for both species across all treatment combinations was 83 ± 4%. Steelhead trout at the highest overall density and California roach enclosed with steelhead at the lower density experienced the highest mean mortality – 29 ± 10% and 31 ± 11%, respectively. Steelhead trout grown at the lowest overall density had the best mean survivorship (94 ± 4%).

Steelhead trout were more aggressive than California roach (Figure 2-12). Steelhead trout attack rates were highest in flowing water and they showed no preference for attacking each other or California roach during the observation periods. Mean steelhead trout intraspecific attack rates in still and flowing water were 3.68 ± 2.55 and 7.93 ± 1.38 attacks per hour, respectively. Steelhead trout attack rates on California roach were 1.92 ± 1.26 in still water and 9.74 ± 2.74 in flowing water. We found no significant differences in California roach intraspecific attack rates between the different habitat types (3.14 ± 1.05

attacks per hour in still water; 4.43 ± 2.61 attacks per hour in flowing water). California roach never attacked steelhead trout.

Feeding behaviors and habitat use varied between species and between flowing and still water. Steelhead trout showed a clear preference for feeding and swimming in flowing water while California roach showed no habitat preferences (Figure 2-13). Rate of water column feeding strikes by both species was higher in flowing than in still water. Additionally, steelhead trout displayed more midwater strikes than California roach. This difference was greatest in flowing water. In contrast, the rate of benthic feeding was highest among California roach. The species also showed a significant difference in their habitat use ($F_{1,18}$=220.3, $p<0.001$). Steelhead trout spent the majority of their time in flowing habitats (mean = 84 ± 3.8%;) while California roach spent their time equally between flowing (53 ± 7.7%) and still habitats (47 ± 7.7%). The experimental treatment combinations had no significant effect on steelhead trout or California roach behavior ($p>0.05$ in all cases). There was also no significant difference in observed behavior between the four different observation bouts per enclosure ($p>0.05$).

The diet mass of steelhead trout grown at the lowest fish density was at least twice as large as the diet masses of steelhead grown under the other treatment combinations (Figure 2-14). However, these differences were not significant after transformation and incorporation of the sequential Bonferroni adjustment. Mean diet mass of steelhead trout at the low densities were 7.14 ± 1.33mg when California roach were present and 14.89 ± 2.75mg when they were absent. At high steelhead trout densities, mean steelhead trout diet mass

was 7.23 ± 3.53mg when California roach were present and 4.96 ± 0.91mg when they were absent. Steelhead trout stomach contents in all enclosures were dominated by macroinvertebrates (overall mean = 84.3 ± 1.3%). Additionally, fifteen of the experimental steelhead trout had post-larval California roach in their stomachs. Mean dried diet mass and percent invertebrates were similar among wild steelhead trout juveniles – 6.27 ± 1.23mg and 86 ± 4.5%, respectively. We found no California roach in the stomachs of wild juvenile steelhead trout.

The dried masses of the California roach foregut contents were similar at the different steelhead trout densities (low steelhead density = 11.11 ± 3.45mg; high steelhead density = 11.91 ± 3.23mg). The combined mean of the foregut content masses for experimental fish was almost 8 times greater than the mean dried masses of wild roach foregut contents (wild = 1.51 ± 0.29mg). Both wild and experimental California roach were omnivorous, with both macroinvertebrates and vegetation each comprising an average of 45% of total diet mass. In one instance, we found a post-larval California roach in the foregut of an experimental roach.

Discussion

Interspecific competition with adult California roach had no measurable effect on YOY steelhead trout growth. However, intraspecific competition had a large effect on steelhead trout growth; steelhead trout gained the most weight in low-density enclosures (Figure 2-11). Our behavioral observations supported these results. Aggressive encounters between steelhead trout and California roach were highly asymmetric – steelhead trout frequently attacked each other and California roach while California roach never attacked steelhead

trout (Figure 2-12). Steelhead trout were most aggressive in flowing water. Our analyses also showed that steelhead trout were equally aggressive toward all fish in the enclosures and showed no preference for attacking each other or California roach. Steelhead trout preferentially fed on invertebrate drift in areas with flowing water while California roach were omnivorous, fed more often on the bottom, and showed no preference for still or flowing water. Taken together, these results suggest that steelhead trout are dominant interference competitors with California roach and that, while there is an overlap in both diet and habitat use, adult California roach do not affect YOY steelhead trout growth.

Both the behavioral and diet data lead us to believe that these experimental results accurately reflect juvenile steelhead trout and adult California roach population dynamics. The high levels of aggression displayed by the experimental steelhead trout were consistent with other published observations of both enclosed and free-swimming individuals (e.g. Hartman 1965, Everest and Chapman 1972, Harvey and Nakamoto 1997, Kelsey et al. 2002). With the exception of post-larval California roach being found in the stomachs of some of the experimental steelhead, the diet mass and composition of the experimental and wild-caught YOY steelhead in our study were virtually identical. Possible explanations for this difference include the effect of the enclosure walls on post-larval roach behavior or a slight shift in steelhead trout feeding behavior due to intraspecific competition or altered post-larval roach behavior.

California roach have been characterized as opportunistic omnivores that display few aggressive behaviors and are prone to displacement by fish predators and more aggressive

fish species (Fite 1973, Moyle 2002). The results from our study agree with these observations; California roach showed no preference for feeding habitat or food type and did not initiate aggressive attacks on steelhead trout. Although the enclosed California roach had more food in their foreguts than the wild fish, their diet composition was nearly identical to that of wild-caught California roach. The differences in diet mass may reflect an increase in food availability for the experimental roach caused by their confinement to a region at the upstream end of a pool that contained high numbers of drifting and benthic food items. Wild fish may have spent more time in the downstream ends of pools where flow, and therefore availability of drifting food items, was lower.

Our results were consistent with the findings of other experiments studying interspecific competition between juvenile steelhead trout and other cyprinids, e.g. rosyside dace (*Clinostomus funduloides*) (Grossman and Boulé 1991), redside shiner (*Richardsonius balteatus*) (Reeves et al 1987), and Sacramento pikeminnow (*Ptychocheilus grandis*) (Reese and Harvey 2002). In each of these studies, juvenile steelhead trout intraspecific aggression was high and the presence of cyprinids did not significantly affect steelhead trout growth at low water temperatures (12-18^{o}C). However, both Reeves et al. (1987) and Reese and Harvey (2002) found that the outcome of the steelhead trout/cyprinid interaction was temperature dependent. In laboratory streams, Reese and Harvey (2002) observed that dominant juvenile steelhead trout received more interspecific attacks, defended smaller territories, and grew less in warm (20-23^{o}C) water and in the presence of Sacramento pikeminnow than when alone in warm water or with Sacramento pikeminnow in colder water. Similarly, Reeves et al. (1987) found that steelhead trout production decreased in

warm water when redside shiners were present. The authors attributed these temperature dependent differences to steelhead trout dominance through interference competition in cold water and redside shiner physiological adaptation and exploitation competition in warm water (Reeves et al. 1987).

The existence of these temperature-based differences in competitive outcome between steelhead trout and sympatric cyprinids is relevant to steelhead trout/California roach dynamics in the Navarro watershed. We have shown that, when grown together under a relatively low temperature regime, California roach does not affect steelhead trout growth. However, since California roach can tolerate water temperatures that induce physiological stress in steelhead trout (Moyle 2002, Werner et al. in prep.), they have the potential to gain a competitive advantage through exploitation competition at elevated water temperatures. Two characteristics of the Navarro drainage make this a potentially significant phenomenon. First, water temperatures in the majority of streams in the Navarro drainage basin are warmer and have larger daily temperature fluctuations than the study reach (J. Feliciano, unpublished data.); stream access, site security, and the lack of baseline data such as we provide here prevented us from attempting our experiment in other areas of the watershed. Second, and most importantly, continuing anthropogenic modification of the stream system and surrounding watershed (e.g. surface and groundwater pumping, forest removal, suburbanization) is creating more stream habitats that are shallower, warmer, less shaded, and thus more favorable for California roach and more stressful for steelhead trout. The increasing preponderance of exposed, warm water environments in the Navarro system

has the potential to negatively affect steelhead trout directly through increased physiological stress and indirectly by giving California roach a competitive advantage.

Steelhead trout/California roach dynamics are further complicated by the fact that competition is not the only way in which these two species could interact. Previous research has shown that the presence of California roach can be beneficial to juvenile steelhead trout. We, and others have observed that YOY and older juvenile steelhead trout prey on both juvenile and adult California roach (Moyle 2002, Power 1990). Furthermore, Tinus and Reeves (2001) found that schools of redside shiners provided a refuge for subdominant steelhead trout from intraspecific aggression. Smaller steelhead gained more mass as redside shiner numbers increased (Tinus and Reeves 2001). Our finding that steelhead trout showed no preference for attacking con-or heterospecifics suggests that the same dilution effect may take place in pools containing different sizes of steelhead trout and schools of California roach. Further field experiments across a wider range of habitats where these two species overlap and using different life history combinations will elucidate the nature of these interactions and how they change in different regions of the watershed.

Given our finding that YOY steelhead trout are negatively affected by high levels of intraspecific competition, it appears that improving YOY steelhead trout habitat would be a suitable restoration and conservation strategy. Increasing habitat availability would reduce both the effects of a density dependent interaction like intense intraspecific competition and the ability of California roach to gain a competitive advantage over YOY steelhead trout. However, increasing the numbers and growth rate of YOY steelhead trout could have a

negative effect on later life history stages; high densities of YOY steelhead trout have been shown to reduce the growth of older juveniles (Harvey and Nakamoto 1997). Furthermore, older juveniles and migrating and spawning adults have different and sometimes conflicting habitat needs than YOY (Moyle 2002). To be effective, steelhead trout conservation strategies must identify which of these habitat types is most severely restricted and how it can be increased while accounting for the strategy's effects on other life history stages and fish community members.

Figure 2-11. Mean steelhead trout growth under the four different treatment combinations. Steelhead trout density had a significant negative effect on steelhead trout growth

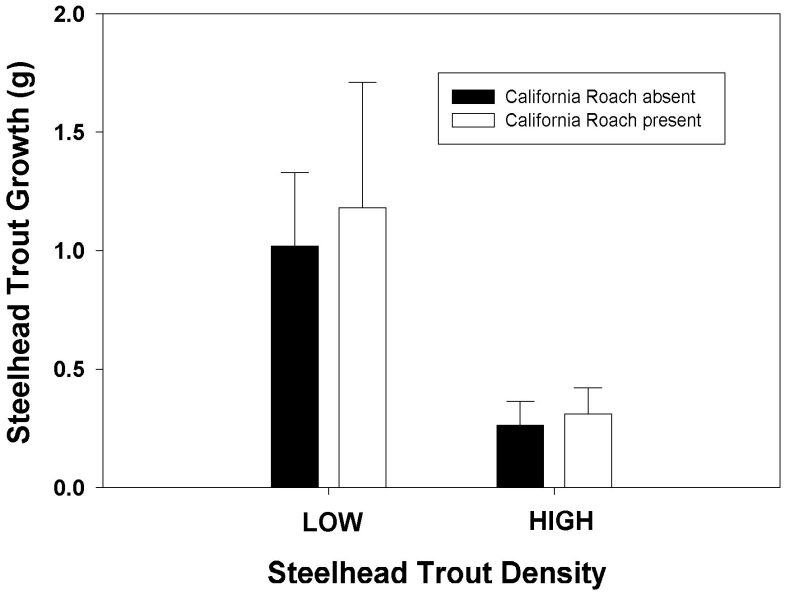

($F_{1,12}$=9.22; p= 0.013) while the presence or absence of California roach did not ($F_{1,12}$=0.23, p=0.64). Error bars are standard error.

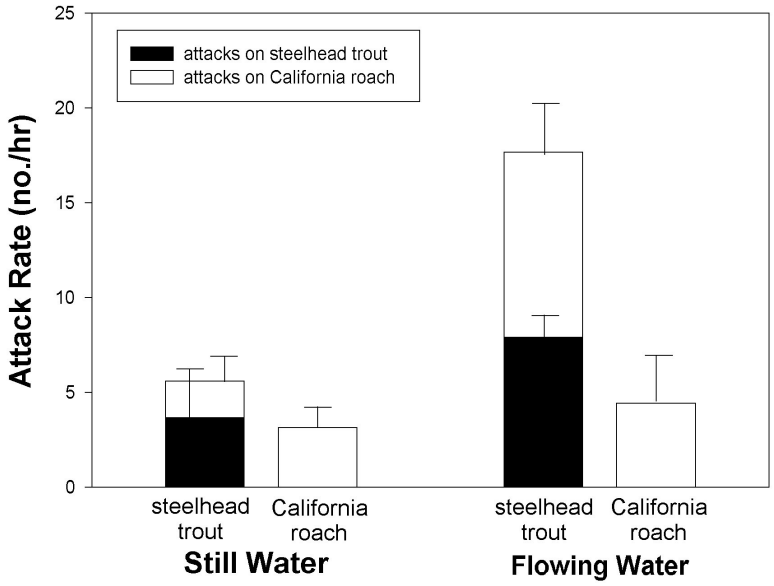

Figure 2-12. Steelhead trout and California roach attack rates, separated by target species and habitat type. Steelhead trout attack rates were significantly higher in flowing versus still water ($F_{1,36}$=8.241, p=0.007). The differences between steelhead trout attack rates on each other and on California roach, when present, were not significant ($F_{1,36}$=1.232, p=0.274). The differences in California roach intraspecific attack rates between the different habitat types were not significant ($F_{1,36}$=0.257, p=0.615). Steelhead trout were never attacked by California roach. Error bars are standard error.

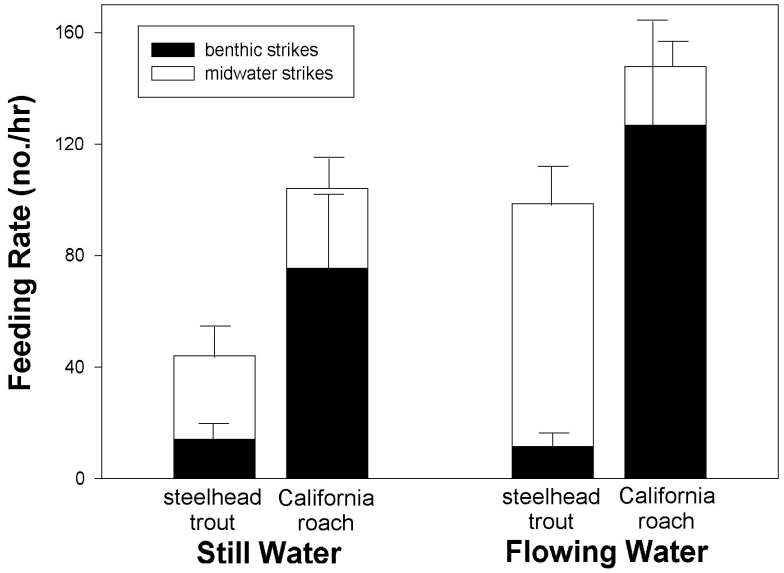

Figure 2-13. Steelhead trout and California roach feeding rates and type (i.e. benthic or water column), separated by habitat type. Steelhead trout made significantly more midwater strikes than California roach ($F_{1,36}$ = 6.573, p=0.015). Both species made more midwater strikes in flowing water ($F_{1,36}$= 11.2, p= 0.002). There was also a significant synergistic interaction effect between species and habitat i.e., steelhead trout made more midwater strikes in flowing water ($F_{1,36}$=11.668, p=0.002). California roach made more significantly more benthic strikes than steelhead trout ($F_{1,36}$=7.605, p=0.009). Habitat type had no significant effect on the rate of benthic strikes for California roach (($F_{1,36}$=0.259, p=0.614)Error bars are standard error.

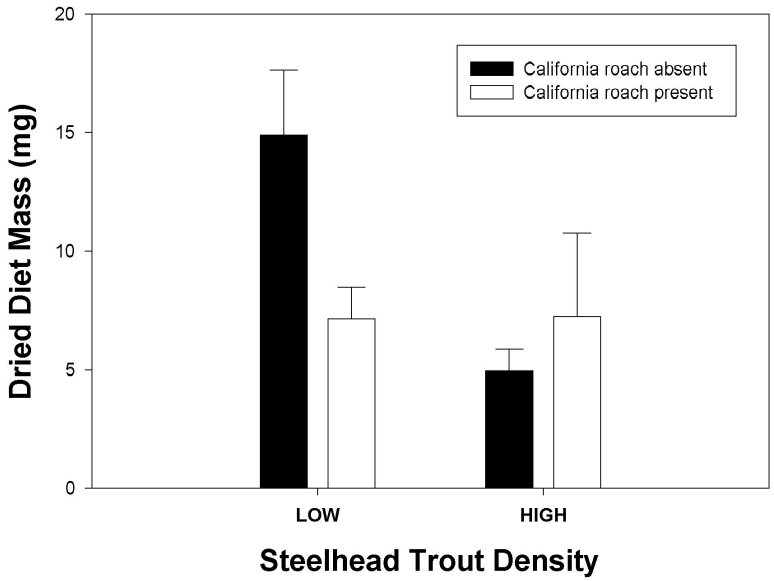

Figure 2-14. Mean dried mass of steelhead trout stomach contents under the four treatment combinations. After data transformation, neither steelhead trout density nor California roach presence/absence had a significant effect on diet mass (steelhead density: $F_{1,12}$=5.28; p=0.04; roach presence/absence: $F_{1,12}$=0.43; p=0.52). Error bars are standard error.

Avian predation in the Navarro River watershed, California

Introduction

The number of piscivorous birds has been increasing in many areas due to both protection of certain species and recovery following human persecuation and pesticide contamination in the mid 1900's (e.g. Hatch and Weseloh 1999). This has led to a renewed interest in the possible effects of avian predators on fish stocks, especially on game fish populations (reviewed in Draulans 1988, Kirby et al. 1996, Cowx in press). Despite the economic importance of the question, whether or not birds impact fish populations remains unclear, with studies finding evidence both ways.

For example, in an early, unreplicated experiment on the Pollet River in Canada, average smolt production increased by 300-500% after trapping out mergansers and kingfishers (Elson 1962). In the Big Qualicum River, on Eastern Vancouver Island, mergansers consumed 24-65% of the smolt production (Wood 1987). Similarly, great cormorants can potentially consume 13-28% of hatchery smolts and 50-65% of wild smolts along an Irish river (Kennedy 1988).

In contrast, double-crested cormorants consumed mostly shad species, and did not have an impact on game fish populations in two lakes in the southeastern United States (Glahn et al. 1998). Kingfishers have also been shown to have no significant impact on game fish in Michigan streams (Salyer and Lagler 1946).

Sometimes different conclusions are reached even when using the same data. Staub et al. (1992, cited in Suter 1995; 1998) concluded that wintering great cormorants were a

significant source of mortality for graylings in Swiss rivers. Using the same data, however, Suter (1995, 1998) concluded that birds were not affecting grayling population dynamics. In other cases, bird predation may even benefit fish populations. Wading birds consumed 76% of fish biomass in an Everglades wetland (Kushlan 1976). However, losses were 93% without avian predation, due to oxygen depletion from the high biomass (Kushlan 1976).

The standard method for assessing the potential for avian predators to impact prey populations is to conduct diet and behavioral studies of the bird species in question, in conjunction with fish population estimates for the area of concern. Results of these studies must be interpreted cautiously, because errors in measuring gut contents, predator abundance, or prey abundance, can lead to problematic results (Kirby et al. 1996). Nevertheless, these types of studies provide a useful initial assessment of whether avian predators can be having significant impacts on fish populations.

One area where all forms of population impacts are a concern are in west coast salmon and trout streams (Brown et al. 1994, Olin 1996, Collis et al. 2002). Many of these streams contain declining population, many listed as threatened or endangered species, with recreational and commercial value (Brown et al. 1994, Collis et al. 2002). To better understand how to protect these species, it is critical that the various factors affecting their basic population biology be understood. This study is part of a larger project attempting to understand the major sources of mortality for salmon and trout in the Navarro River watershed.

There are three periods when predation by terrestrial predators could be important: when salmon are in-migrating, when salmon are out-migrating, and during summer low-flow periods. During the two stages of migration, fish abundance is higher, and all migrating fish must pass through the estuary, a potential bottleneck that can attract large numbers of predators. One study examined avian predation during out-migration on the Columbia River, and found that throughout most of the watershed avian predators were having a negligible impact, with the exception of certain portions of the estuary (Collis et al. 2002). During late summer, flows are reduced, depths decrease, and a larger percentage of the habitat is available to terrestrial predators, limited in their foraging efficiency by water depth and flow during other periods of the year.

This study focused on the potential predator impact during the summer low flows. Because of the threatened and endangered status of the steelhead and Coho in these streams, limiting the possibilities for manipulative experiments, we took an observational approach to assessing the potential impact of avian predators. (In addition to birds, river otters are another potential terrestrial predator. However, we found otter scat throughout the watershed that indicated that during the course of our study they were consuming almost exclusively crayfish, and thus are not considered further here.) By conducting a series of bird and fish surveys, along with bird foraging observations, we will assess the potential impacts of avian predators on fish populations throughout the Navarro river watershed.

Methods

This study was conducted from 16 June to 30 July 2001 in the Navarro River watershed, Mendicino County, CA, USA. To assess the potential impacts of avian predators, we: 1)

conducted bird surveys throughout the watershed to assess predator abundance, 2) conducted behavioral observations at selected locations throughout the watershed to assess predation rates, and 3) conducted seining and snorkeling surveys to assess fish abundance.

Site Description

The most abundanct piscivorous birds in the watershed include: great blue herons (*Ardea herodias*), green herons (*Butorides virescens*), belted kingfishers (*Ceryle alcyon*) and common mergansers (*Mergus merganser*). A number of additional avian piscivores are found at the estuary, including double-crested cormorants (*Phalacrocorax auritus*), osprey (*Pandion haliaetus*), brown pelicans (*Pelecanus occidentalis*), and caspian terns (*Sterna caspia*).

Bird Surveys

We conducted behavioral observations along 14 sections of stream throughout the watershed. The sites were chosen to represent a variety of stream types, from both arid headwaters, to heavily vegetated headwaters, to open medium sized streams, to the main stem of the Navarro River, to the estuary. Sites were also chosen to overlap with pre-existing sampling locations as much as possible. Sites ranged in length from 1.67 km for upper watershed sites which were close together to 8 km for the main stem of the Navarro, with most sites surveyed for 5 km. We conducted line transect surveys (Bibby et al. 2000), with the streambed serving as our transect line. The surveyor walked (upper wateshed sites) or kayaked (main stem and estuary sites) the length of the stream, making note of any birds observed along the transect. If there was any uncertainty about whether a bird was a new bird, or one that had been chased ahead by the observer, the bird was not counted as a new bird. In most cases, however, it was clear when the bird circled around

behind the observer, making us confident that any other birds cited were new birds. Surveys took about one week to complete and were conducted at the start of the experiment in mid-June, and again at the completion in late July.

Behavioral observations

Behavioral observation were conducted at 5 locations throughout the watershed, ranging from headwaters, to medium size streams, to the main stem, to the estuary, thus covering a gradient in stream order and drainage area. Each site was watched for 4-5 days, with a target of 35 hours of observation per site. Observations were conducted unless there was rain or extremely heavy and persistent fog in the estuary. Observations were conducted from a camouflaged blind using 8x32 Nikon binoculars. We noted bird species present, time each species was present, and number of attacks and kills per species.

Mark-Recapture Study

A mark-recapture study was conducted in the estuary during early September 2001. Although this study was conducted over a month after the bird observations ended, we still feel the information can provide some insight into potential impacts. We used the program NOREMARK (White 1996) to estimate population abundance.

Impact Estimates

We used the four locations where we had both predation rates and fish densities to assess the potential impact of avian predators. Assuming that most of the avian predators are feeding primarily during daylight hours, we calculated the number of prey consumed between fish surveys as follows:

Prey consumed between fish surveys = # prey/hour/km x length of study reach x 14.5 hours (average daylength) x days between surveys

The resulting number was then divided by the total June fish estimate for the study reach to obtain the percent of prey consumed by birds for that reach. We looked at overall predation rate, as well as estimated impacts on individual species. Although we have no quantitative data on diets of these predators, previous diet studies indicate that avian predators feed on prey based on their relative abundance (Butler 1992, Hamas 1996, Hatch 2000). Therefore, to estimate impacts, we first assumed birds were eating prey in proportion to their relative abundance, and calculated the number of prey consumed accordingly. We also considered a worst-case scenario where prey consumed exclusively 0+ age class steelhead. Finally, by subtracting the July steelhead estimate from the June steelhead estimate we obtained the total decrease in this size class in the 7 week period between fish surveys and calculated what percent of this decrease could be attributed to avian predation. Coho and other age classes of steelhead were not considered in the estimates due to their low numbers.

In general, the number of bird species increases with stream order and drainage area. We used a regression approach to see if this generalization was true for the Navarro, and if we could predict predator density based on drainage area. Other factors controlling avian predator effectiveness include depth (Salyer and Lagler 1946, Butler 1992, Hatch and Weseloh 1999) and temperature (Kramer et al. 1983). Nine of the sites had additional information available on average depths, daily temperature profiles, and fish densities. We

determined the maximum temperature for each day between our avian predator surveys, and from these calculated an average maximum daily temperature for these sites. We then used a multiple regression approach, with a backwards-stepwise procedure, to examine the effects of average maximum daily temperatures, average depth, fish density, and drainage area on avian predator densities. Predator densities were log(x+1) transformed to meet the assumptions of the tests.

Results

The overall predator density generally increased moving downstream (Table 2-6, Table 2-7), and this pattern was significantly associated with drainage area (r^2=0.709; $F_{1,12}$=29.22; p<0.001; Figure 2-15). As drainage area increased, the number of bird predators increased. Heavily forested headwater sites had no predators; more open headwater sites consistently had kingfishers, and occasionally a green or great blue heron. Green and great blue herons become more ubiquitous further downstream, and some common mergansers were found in medium sized streams. Finally, at the estuary there were increased numbers of mergansers, as well as an occasional double-crested cormorant, an osprey, and caspian terns. Brown pelicans were also occasionally seen, but were never observed feeding in the estuary; they seemed to prefer to forage just offshore.

Unfortunately, there was no temperature, depth, and/or fish abundance estimates available for many of the larger sites (notably the estuary, main stem, and lower Rancheria Creek, the areas with the largest drainage area), so we ran a multiple regression on a subset of the data consisting of the small and medium sized streams within the watershed. The overall regression was significant (r^2=0.876, $F_{3,5}$=11.763; p=0.011). The backward selection

stepwise procedure selected average maximum daily temperature ($t_{1,5}$=7.742, p=0.039), maximum depth ($t_{1,5}$=15.011; p=0.012), and fish density ($t_{1,5}$=10.613; p=0.022) as significant variables in the model (Figure 2-16). Despite the significant affect in the previous regression, drainage area was not selected in this model ($t_{1,5}$=0.496; p=0.632). Notice that both regressions are significant even when using a Bonferroni correction for running two regressions (i.e. both are significant at alpha = 0.025).

Actual predation rates showed a different pattern. When expressed as mean number of kills per hour (Figure 2-17) or as mean number of kills per day per km of stream length (Table 2-6), predation rates appear to increase as you move down stream (Table 2-6, Figure 2-17). However, when predation rates are expressed as mean number of kills per day per area, this trend disappears (Figure 2-18). Thus with the exception of the estuary, most of the watershed has similar predation rates. Upper sites have lower predator densities and lower predation rates per unit time at a given point, but predators are also foraging on narrower and shallower areas, stretched over a greater distance. Much of the increased predation rate at the estuary was due to a flock of 40 mergansers roosting on a large snag in the estuary. The mergansers would regularly forage in the lower portion of the estuary, although they also clearly dispersed upstream to forage through part of the day.

We were able to compare our predation rates with four sites that had information on fish abundance. Snorkeling surveys were available for the mid to upper watershed sites, and mark-recapture information was available for steelhead trout in the estuary. No fish information was available for the main stem site. Assuming birds were consuming fish

species in relation to their relative abundance, avian predators could consume less than 3% of the total fish stocks between the two snorkeling surveys (Table 2-8), with relatively few individuals of any species being consumed (Table 2-18).

For the lower portion of the estuary, we marked a total of 190 fish, and recaptured 25. Only two fish were captured more than once, and both were recaptured at the same sampling station at which they were tagged. We estimated the population estimate for the lower portion of the estuary to be 2,410 steelhead, with 95% confidence intervals ranging from 1,727-3,566. If predation rates are similar in early September to those in late July, then birds can consume 35 prey per hectare per day (Figure 2-18). Since the lower half of the estuary is approximately 4 hectares, this means that 140 prey were consumed in the lower estuary per day.

Discussion

Avian predation does not appear to be a critical source of direct mortality for coho, salmon, or other fish species throughout much of the Navarro watershed. Predator densities are below 2/km throughout most of the watershed, although densities increase to 32.5/km at the estuary (Table 2-6). Predation rates also appear to be fairly low in most locations, with birds consuming less than 3% of the total number of fish from early June to late July in the mid and upper portions of the watershed.

It appears extremely unlikely that avian predators are having a significant impact on the steelhead or coho in this watershed. Most bird species feed on the most abundant prey species, and show no selectivity for given species (Butler 1992, Hamas 1996, Hatch 2000).

Older steelhead and coho occur in such low densities that birds are not likely to be cueing in on them as prey, but rather consuming mostly the more abundant 0+ steelhead, California roach, and three-spined sticklebacks (Table 2-8). Assuming birds are consuming prey in relation to their densities, birds account for at most 8% of the decrease in this size class from June to July (Table 2-9). In a worst-case scenario where birds are foraging exclusively on 0+ steelhead, they still only account for between 8-21% of decreased numbers between June and July (Table 2-9). Although we do not have information on the diets of birds during out study, previous diet studies indicate that this later scenario is extremely unlikely, and that the former is a more realistic assessment of potential impacts. If anything, predation rates are likely to be lower than these estimates. A previous experiment indicated that young steelhead spend more time in riffles than pools (J. B. Feliciano, unpubl data), where water turbulence makes most birds less effective predators (e.g. Sayler and Lagler 1946).

The one place where predation may be an important source of mortality is at the estuary. The estuary contains the largest density of predators, drawing both oceanic and freshwater species. We estimated that birds could consume 140 prey per day in the lower part of the estuary (approximately 4 hectares in area). Thus in one month birds could potentially consume 4,200 fish, or 174% of the fish in the estuary. Since this is clearly not the case, birds either consume substantial numbers of alternative prey not included in the steelhead mark-recapture study, there is significant recruitment occurring, there is substantial immigration, or some combination of these. In fact, seine hauls indicate that from May to August, during our study, the average number of steelhead, and other fish caught per seine

haul actually increased (R. Bush, unpubl. data). Pulling a 30.54m seine in a half circle from the shore (5,837m^2) yielded an average of 7.67 steelhead in May, but 24.6 in August. Also, no three-spined sticklebacks were caught in May, but an average of nine per seine haul were caught in August. This indicates that although there is the potential for significant predation on steelhead, the population is increasing in numbers through the early part of the summer. The addition of new prey items, such as the stickleback, through recruitment, most likely help buffer effects on steelhead. The potential for a substantial increase through immigration appear to be minimal for this time of year. The upper portions of the watershed have very low flows, and are frequently drawn down to isolated pools connected by very shallow riffles. Further supporting the limited movements during summer drawdowns, two steelhead that were recaptured twice were caught at the same station at which they were marked.

Whether or not the predation that is occurring is having a significant impact on the coho or steelhead remains unclear. This depends in large part on whether the predation is regulatory or compensatory. And this question is impossible to answer without knowing more about sources of mortality during both the terrestrial and oceanic portions of their life history. Current knowledge of the terrestrial portion of the life history in the Navarro watershed indicates that July-October is the period of highest mortality for coho and steelhead (M. Johnson, unpubl. data). Low flows and high temperatures appear to be the major source of mortality during this time. Under these conditions, terrestrial predation is likely mostly compensatory, or potentially even beneficial by thinning fish numbers and

preventing larger losses due to anoxic conditions and resource depletion. Such a situation has been shown to occur in an Everglades pond (Kushlan 1976).

The most common technique for assessing avian impacts on fish populations is to conduct diet studies of predators, determine the sizes and numbers of prey consumed, and compare these numbers with fish population estimates to determine the potential impact. This technique can work quite well for lakes, ponds or reservoirs where the predators feed exclusively on that area, or when studying birds foraging within clearly defined territories. However, if predators forage over larger areas, then simply knowing how many prey are consumed says nothing about how their foraging is dispersed across the landscape. For example, double-crested cormorants can forage up to 60km from their night roosts, with an average distance of 15km, and travel an average of 5.6km between foraging sites (King et al. 1995, Hatch et al. 2000). Similarly, great blue herons can forage up to 15km from their nesting sites (Gibbs 1991). For animals foraging along streams, an individual predator disperses its foraging effort over long stretches of stream, reducing the impact on fish located within specific reaches. The same is true for predators moving among multiple wetlands, ponds, or lakes. Therefore, in areas where predators routinely forage over a large area, we believe that knowing the predation rate per unit time per unit area gives a better predictor of impacts on fish stocks. A number of studies have published biomass estimates of bird impacts on fish stocks, but again, most of these are based on the assumption that birds are foraging exclusively on the water body in questions, which is not always clearly the case.

While there are numerous diet studies of most of the birds encountered in this study, surprisingly few other studies report predation rates for piscivorous avian predators in terms of numbers of prey consumed per some time unit. With the exception of one study in which one of us was involved (Steinmetz et al. in press), no other studies that we are aware of report predation rates per unit area per unit time. A few other studies used focal animal observation and report predation rates per unit time, and these are summarized in Table 2-11. (Since they are not directly comparable to our study, we have not listed the number of studies that report impacts on biomass per unit area.) Our study found generally lower predation rates than the others (Table 2-10). A number of these studies were conducted at hatcheries and fish farms, where there is undoubtedly a higher predation rate due to higher densities of prey. Similarly, one study in Illinois streams probably found higher predation rates due to the higher productivity of these warmwater Midwestern streams.

Conclusions

In summary, predator density generally increased with increasing drainage area, while predation rates remained fairly constant through much of the watershed. Predation rates increased dramatically at the estuary, due to an increase in predator density, particularly mergansers. Avian predation does not appear to be a major source of mortality (<3%) throughout much of the watershed, with the exception of the estuary, where the potential exists for substantial predation on steelhead and coho. However, effects on the population appear to be minimal as the population appeared to increase during the period of our study. If predation in the estuary becomes a management concern, two simple solutions would be to remove potential roosting sites for mergansers and/or actively scare predators away

during critical parts of the year (e.g. in- and out-migration). Future studies should examine the effects of these predators during in- and out-migration.

Table 2-6. Avian Predator Densities and Predation Rates in the Navarro River Watershed (all species combined)

Stream	Site	Max # Observed	Distance Surveyed	Predator Density (# predators /km)	Drainage Area	Predation Rates (# prey/day/km)
Flynn	LFC	0	1.67	0		NA
Flynn	MFC	0	1.67	0		NA
Flynn	UFC	0	1.67	0		NA
North Fork	UNF	0	5	0		NA
Rancheria	URC	1	5	0.2		NA
Anderson	MAC	1	5	0.2		NA
North Fork	LNF	2	5	0.4		NA
Anderson	UAC	3	5	0.6		5.3
North Fork	MNF	3	5	0.6		6.1
Indian	MIC	4	5	0.8		NA
Indian	LIC	4	5	0.8		NA
Rancheria	LRC	9	5	1.8		8.3
Main Stem	MST	16	8	2		16.8
Estuary	EST	52	1.6	32.5		370.7

Table 2-7. Individual Species Densities in the Navarro River Watershed

Stream	Site	Distance Surveyed	GBH	#/km	GH	#/km	BKF	#/km	CM	#/km	DCC	#/km	OSP	#/km	TRN	#/km
Flynn	LFC	1.67	0	0	0	0	0	0	0	0	0	0	0	0	0	0
Flynn	MFC	1.67	0	0	0	0	0	0	0	0	0	0	0	0	0	0
Flynn	UFC	1.67	0	0	0	0	0	0	0	0	0	0	0	0	0	0
North Fork	UNF	5	0	0	0	0	0	0	0	0	0	0	0	0	0	0
Rancheria	URC	5	1	0.2	0	0	0	0	0	0	0	0	0	0	0	0
Anderson	MAC	5	0	0	0	0	1	0.2	0	0	0	0	0	0	0	0
North Fork	LNF	5	0	0	1	0.2	1	0.2	0	0	0	0	0	0	0	0
Anderson	UAC	5	1	0.2	1	0.2	1	0.2	0	0	0	0	0	0	0	0
North Fork	MNF	5	1	0.2	1	0.2	1	0.2	0	0	0	0	0	0	0	0
Indian	MIC	5	0	0	1	0.2	3	0.6	0	0	0	0	0	0	0	0
Indian	LIC	5	0	0	1	0.2	3	0.6	0	0	0	0	0	0	0	0
Rancheria	LRC	5	0	0	1	0.2	3	0.6	0	0	0	0	0	0	0	0
Main Stem	MST	8	1	0.13	2	0.25	4	0.5	8	1	0	0	1	0.13	0	0
Estuary	EST	1.6	1	0.63	0	0	2	1.3	40	25	2	1.3	1	0.63	6	3.8

GBH=great blue heron; GH=green heron; BKF=belted kingfisher; CM=common merganser; DCC=double-crested cormorant; OSP=osprey; TRN=caspian tern

Table 2-8. Estimated Impacts on Fish Populations

Site	Kills/day /km	Length of Study Reach	Total # kills/day	Time Between Surveys (days)	# Fish consumed	June Fish Estimate	
						Total	%consumed
Estuary	358.7						
Lower Rancheria	8.26	0.307	2.53582	49	124.25518	5520	0.02251
Middle North Fork	6.47	0.148	0.95756	49	46.92044	1790	0.026213
Upper Anderson	5.46	0.126	0.68796	51	35.08596	708	0.049556

Table 2-9. Estimated Numbers of Major Fish Species Consumed by Birds from Early June to late July*

Site	June Fish Estimate											
	Total 0+STH	Estimated # Eaten	Total 1+ STH	Estimated # Eaten	Total Ad STH	Estimated # Eaten	Total Coho	Estimated # Eaten	Total CAR	Estimated # Eaten	Total 3SS	Estimated # Eaten
Estuary												
Lower Rancheria	884	19.9	3	0.068	0	0	0	0	4621	104	11	0.25
Middle North Fork	547	14.3	11	0.29	0	0	20	0.52	720	18.9	492	12.9
Upper Anderson	704	34.9	1	0.05	3	0.15	0	0	0	0	0	0

*Estimates based on birds consuming prey in proportion to their abundance at each site. Abbreviations as follows: 0+STH=steelhead, 0+ age class; 1+STH=steelhead, 1+ age class; Ad STH=steelhead, adult; Coho=coho salmon; CAR=California roach; 3SS=three-spined stickleback

Table 2-10. Estimated Percent 0+Steelhead Mortality Attributable to Birds

Site	June 0+ Estimate	July 0+ Estimate	Change	Proportional Estimate *	% change due to birds	Maximum Estimate†	% change due to birds
Estuary							
Lower Rancheria	884	289	595	19.9	3.3%	124.3	20.9%
Middle North Fork	547	235	312	14.3	4.6%	46.9	15.0%
Upper Anderson	704	260	444	34.9	7.9%	35.1	7.9%

* Estimates based on birds consuming prey in proportion to their abundance

† Birds feed only on 0+Steelhead

Table 2-11. Predation Rates of Avian Predators in the United States

Predator	Predation Rate (#/hour)	Predation Rate (#/time/area)	Location	Source
Belted Kingfisher	1.7 trout/hour	NA	Hatcheries in northeastern U.S.	Glahn et al. 1999
Belted Kingfisher	0.10 prey/hour	20.8 prey/day/hectare	Northern Illinois, USA	Steinmetz et al. in press
Belted Kingfisher	*0-0.46 prey/hour*	*0-18.9 prey/day/hectare*	*Northern California watershed*	*This study*
Great Blue Herons	2.2 trout/hour	NA	Hatcheries in northeastern U.S.	Glahn et al. 1999
Great Blue Herons	0.14 catfish/hour	NA	Catfish ponds at the National Wildlife Research Center in Mississippi, USA	Glahn et al. 2000
Great Blue Herons	0.8 catfish/hour	NA	Catfish farms in Mississippi, USA	Stickley et al. 1995
Great Blue Herons	0.07 prey/hour	13.6 prey/day/hectare	Northern Illinois, USA	Steinmetz et al. in press
Great Blue Herons	*0-0.20 prey/hour*	*1.5-1.9 prey/day/hectare*	*Northern California watershed*	*This study*
Green Herons	3.1 trout/hour	NA	Hatcheries in northeastern U.S.	Glahn et al. 1999
Common Merganser	*9.6 prey/hour*	*34.83 prey/day/hectare*	*Northern California estuary*	*This study*
Double-crested Cormorant	5 catfish/hour		Catfish farms in Mississippi, USA	Stickley et al. 1992
Double-crested Cormorant	*0.04 prey/hour*	*0.13 prey/hectare/day*	*Northern California estuary*	*This study*
Osprey	2.1 trout/hour	NA	Hatcheries in northeastern U.S.	Glahn et al. 1999
Osprey	*0.25 prey/hour*	*0.11 prey/hectare/day*	*Northern California estuary*	*This study*
Caspian Tern	*0.07 prey/hour*	*0.47 prey/hectare/day*	*Northern California estuary*	*This study*

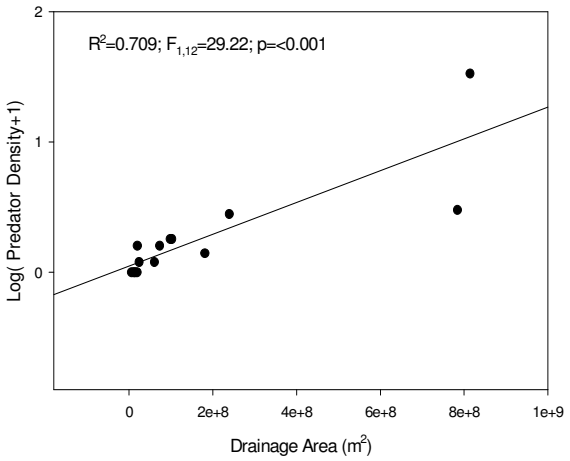

Figure 2-15. Relationship between drainage area (m^2) and predator density (#/km) for the Navarro River watershed, northern California, USA. *(Note: this figure does not yet include all sites – still working out a discrepancies in a few sites, including the estuary.)*

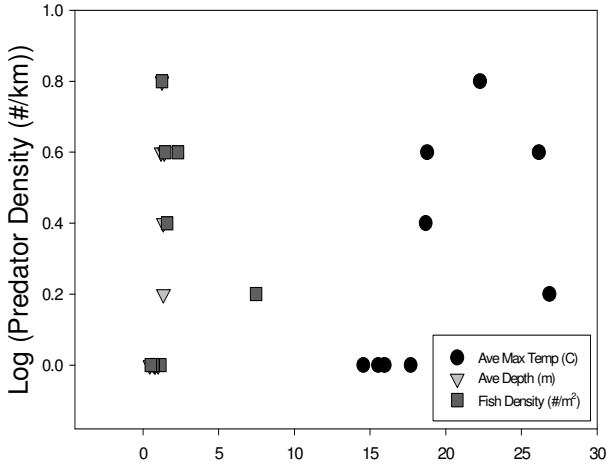

Figure 2-16. Relationship between average daily maximum temperature, average depth, and fish density and log(avian predator density +1). All three variables were significant in a multiple regression.

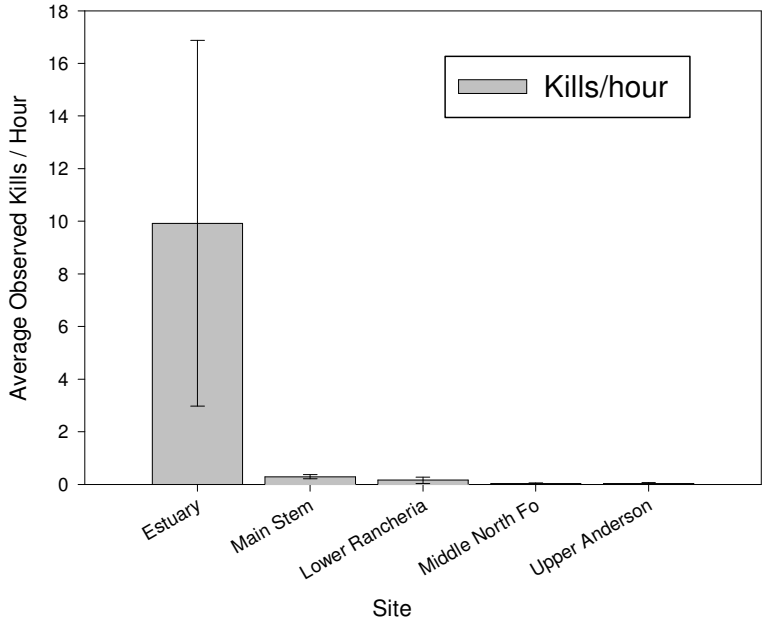

Figure 2-17. Predation rates at five sites, moving from the estuary (left) up through the watershed (right). Rates expressed as number of kills per hour. Error bars are ± 1 SE.